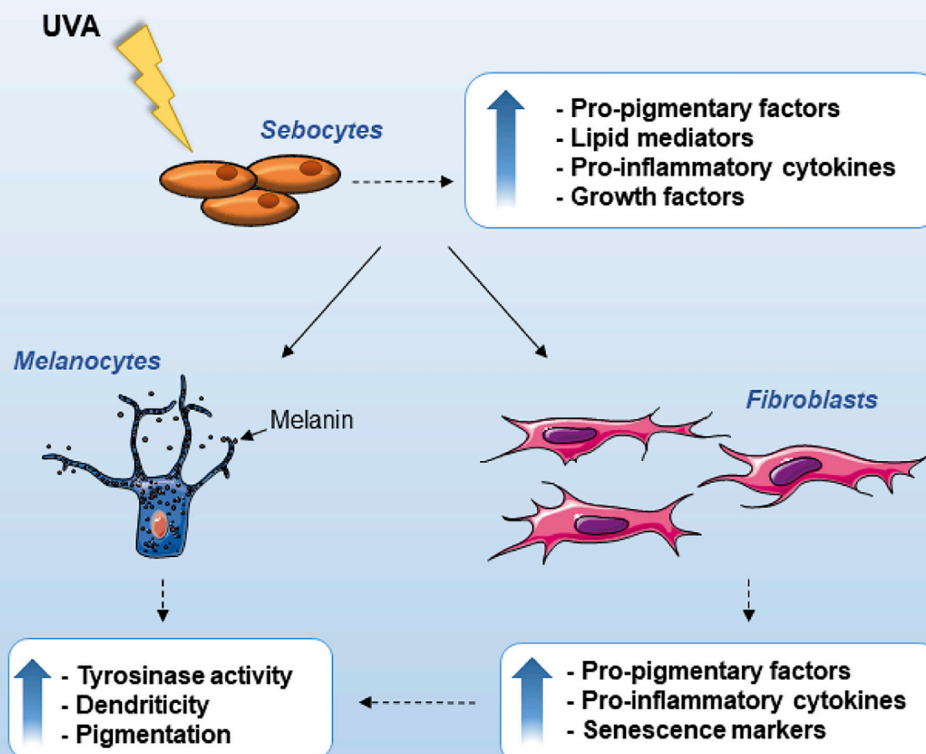


## Article

## Sebocytes contribute to melasma onset

**Involvement of sebocytes in melasma**

Enrica Flori,  
Arianna  
Mastrofrancesco,  
Sarah Mosca, ...,  
Marco Zaccarini,  
Christos C.  
Zouboulis, Mauro  
Picardo

enrica.flori@ifo.it (E.F.)  
mauro.picardo@hotmail.it  
(M.P.)

**Highlights**  
Irradiated sebocytes  
produce and upregulate  
the factors  $\alpha$ -MSH, EDN1,  
SCF, and b-FGF

Sebocyte-derived factors  
drive modifications of  
fibroblasts and  
melanocyte behavior

Sebocytes participate in  
the skin cells cross-talk  
regulating pigmentation

Sebocytes locally support  
the inflammatory and  
photo-aged environment  
in melasma

Flori et al., iScience 25, 103871  
March 18, 2022 © 2022 The  
Authors.  
<https://doi.org/10.1016/j.isci.2022.103871>



## Article

## Sebocytes contribute to melasma onset

Enrica Flori,<sup>1,5,\*</sup> Arianna Mastrofrancesco,<sup>1,5</sup> Sarah Mosca,<sup>1</sup> Monica Ottaviani,<sup>1</sup> Stefania Briganti,<sup>1</sup> Giorgia Cardinali,<sup>1</sup> Angela Filoni,<sup>2</sup> Norma Cameli,<sup>2</sup> Marco Zaccarini,<sup>3</sup> Christos C. Zouboulis,<sup>4</sup> and Mauro Picardo<sup>1,6,\*</sup>

## SUMMARY

Melasma is a hyperpigmentary disorder with photoaging features, whose manifestations appear on specific face areas, rich in sebaceous glands (SGs). To explore the SGs possible contribution to the onset, the expression of pro-melanogenic and inflammatory factors from the SZ95 SG cell line exposed to single or repetitive ultraviolet (UVA) radiation was evaluated. UVA up-modulated the long-lasting production of  $\alpha$ -MSH, EDN1, b-FGF, SCF, inflammatory cytokines and mediators. Irradiated SZ95 sebocyte conditioned media increased pigmentation in melanocytes and the expression of senescence markers, pro-inflammatory cytokines, and growth factors regulating melanogenesis in fibroblasts cultures. Cocultures experiments with skin explants confirmed the role of sebocytes on melanogenesis promotion. The analysis on sebum collected from melasma patients demonstrated that *in vivo* sebocytes from lesional areas express the UVA-activated pathways markers observed *in vitro*. Our results indicate sebocytes as one of the actors in melasma pathogenesis, inducing prolonged skin cell stimulation, contributing to localized dermal aging and hyperpigmentation.

## INTRODUCTION

Melasma is a common hyperpigmentary disorder mainly affecting women of childbearing age, manifested as asymptomatic light to dark brown spots, with irregular edges in the photo-exposed areas, mainly on the face (Cario 2019; Del Bino et al., 2018; Handel et al., 2014a; Kwon et al., 2019; Passeron and Picardo 2018). The pathology is considered a consequence of female hormone stimulation on a predisposed genetic background although other players are involved in the onset as well (Kwon et al., 2019; Passeron and Picardo 2018; Ortonne et al., 2009). Exposure to solar radiation is the most triggering environmental factor and UVB, UVA, and the shorter wavelengths of visible light contribute to hyperpigmentation. Broad UV sunscreens including filters for blue light reduce intensity and recurrence of the manifestation (Boukari et al., 2015; Duteil et al., 2014; Handel et al., 2014b; Lakhdar et al., 2007; Regazzetti et al., 2018). Histologically, the lesions are characterized by basal membrane modifications, presence of pendulous melanocytes (Lee et al., 2012), solar elastosis, and increased dermal mast cells and blood vessels, leading to the inclusion of melasma among the photo-aged disorders (Kwon et al., 2016, 2019; Passeron and Picardo 2018; Hernandez-Barrera et al., 2008; Kang et al., 2002; Kim et al., 2007; Torres-Alvarez et al., 2011). Keratinocyte-derived and fibroblast-derived paracrine melanogenic factors are overexpressed, indicating the relevant role of these cells in the pathogenesis linked with an impairment in the intercellular network (Torres-Alvarez et al., 2011; Bak et al., 2009; Byun et al., 2016; Chen et al., 2010; Hasegawa et al., 2015; Im et al., 2002; Kang et al., 2006; Kapoor et al., 2020; Miot et al., 2010; Wang et al., 2017).

Melasma appears more frequently on specific face areas, such as the malar, forehead, and upper lips, rich in sebaceous glands (SGs). SGs synthesize and produce sebum (Kurokawa et al., 2009; Makrantonaki et al., 2011), and possess metabolic, neuroendocrine, and immunological functions, participating in the multicellular communication network underlying skin homeostasis (Clayton et al., 2020; Picardo et al., 2015; Szollosi et al., 2018; Zouboulis et al., 2016). SGs express several hormonal receptors including the melanocortin receptors, 1 (MC-1R) and MC-5R (Bohm et al., 2002), and secrete several cytokines, hormones, and vitamins that modulate the morphology and functions of skin cells including melanocytes. Body regions rich in sebocytes, such as the face, axillae, and genitalia, exhibit the

<sup>1</sup>Laboratory of Cutaneous Physiopathology and Integrated Center of Metabolomics Research, San Gallicano Dermatological Institute, IRCCS, Rome, Italy

<sup>2</sup>Dermatology Department, San Gallicano Dermatological Institute, IRCCS, Rome, Italy

<sup>3</sup>Genetic Research, Molecular Biology and Dermatopathology Unit, San Gallicano Dermatological Institute, IRCCS, Rome, Italy

<sup>4</sup>Departments of Dermatology, Venereology, Allergology and Immunology, Dessau Medical Center, Brandenburg Medical School Theodore Fontane and Faculty of Health Sciences Brandenburg, Dessau, Germany

<sup>5</sup>The authors contributed equally

<sup>6</sup>Lead contact

\*Correspondence:  
enrica.flori@iof.it (E.F.),  
mauro.picardo@hotmail.it (M.P.)

<https://doi.org/10.1016/j.isci.2022.103871>



highest melanocyte density and pigmentation level (Bolognia and Pawelek 1988). Moreover, the coculture of the human SG cell line SZ95 and melanocytes promotes melanocyte proliferation and dendricity (Abdel-Naser et al., 2012); in addition, UV-oxidized skin surface lipids, particularly squalene, induce melanocyte proliferation and melanin synthesis in organ tissue cultures (Picardo et al., 1991).

To evaluate whether sebocytes contribute to generate growth factors and other mediators participating to the melasma appearance, SZ95 sebocytes, an *in vitro* reliable model to study human sebocyte physiopathological aspects (Schneider and Zouboulis 2018; Zouboulis et al., 1999), were irradiated with different doses of UVA, able to reach the dermis and skin appendages, thus participating in skin aging and melasma onset (Mahmoud et al., 2010). After a single and repeated exposure, the growth factors and inflammatory mediator's production were evaluated. Moreover, the conditioned media from irradiated sebocytes were added to melanocytes and fibroblasts cultures to investigate the capability to modulate their functions. *Ex vivo* skin explants cocultures with SZ95 sebocytes and sebum evaluations were performed to demonstrate the relevance of the *in vitro* findings.

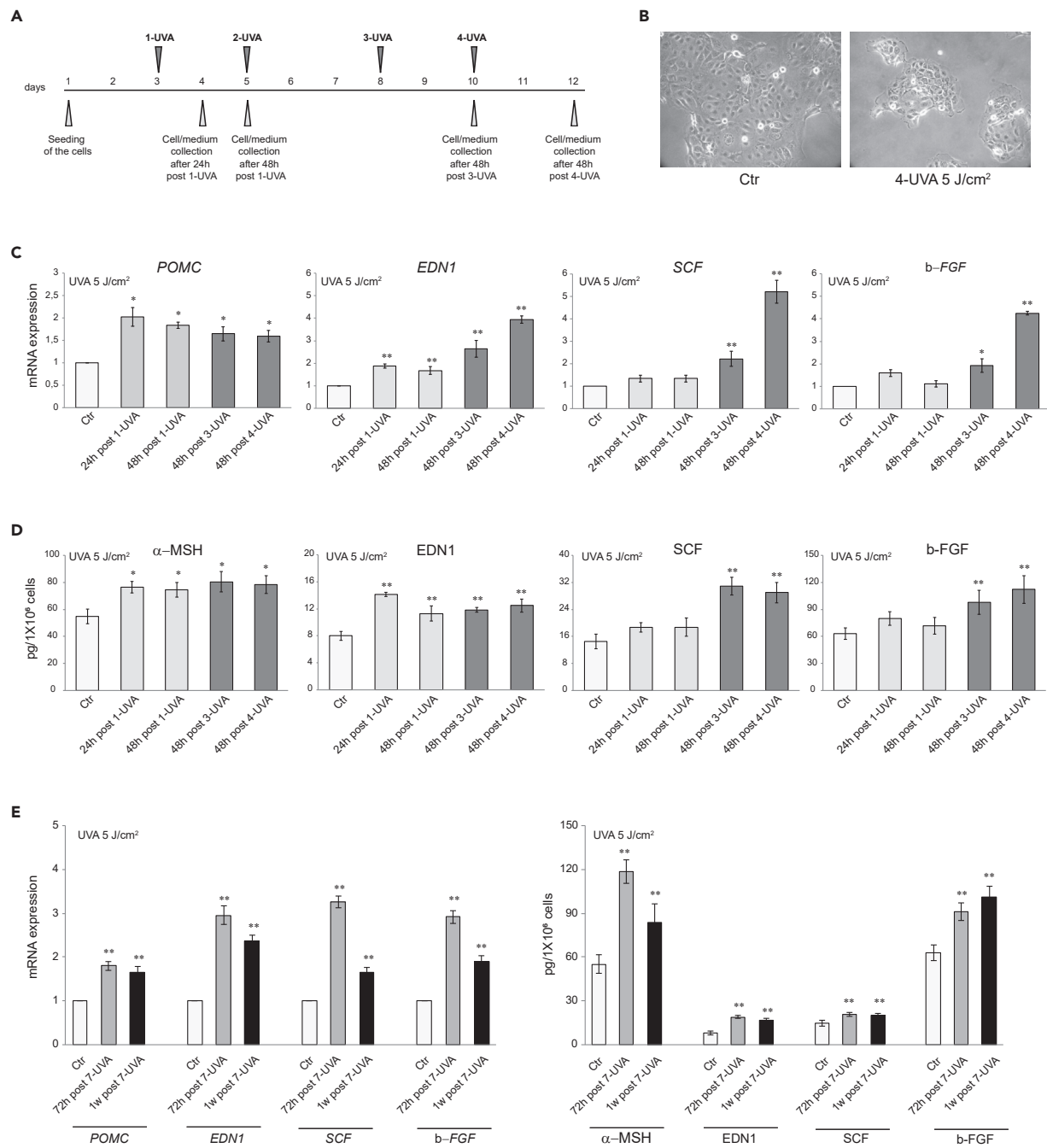
## RESULTS

### UVA irradiation of SZ95 sebocytes induces a release of growth factors, cytokines, and lipid molecules

Because sebocytes and keratinocytes originate from the same stem cells (Toth et al., 2011), we asked whether SZ95 sebocytes, following UVA exposure, produce pro-melanogenic factors as keratinocytes do (Hirobe 2005; Imokawa 2004; Lo Cicero et al., 2015; Murase et al., 2009). As repeated exposure of human dermal fibroblast to 6 J/cm<sup>2</sup> UVA was suitable to mimic the *in vivo* doses inducing photoaging (Lan et al., 2019), SZ95 cells were irradiated with 5 J/cm<sup>2</sup> UVA, according to the scheme in Figure 1A. UVA exposure influenced SZ95 cell morphology, resulting in progressive enlargement, exacerbated polymorphous appearance, different sizes, and increased cytoplasmic protrusions (Figure 1B). A cell number reduction was noted after repeated UVA irradiation (30 ± 5% vs Ctr). Increased expression of POMC, encoding a precursor of α-MSH, and EDN1 genes was observed. The protein analyses confirmed the significant production, after a single 5 J/cm<sup>2</sup> UVA, of these two major melanogenic factors normally produced by keratinocytes after UV exposure (Figures 1C and 1D). The effect size of α-MSH induction after a single UVA exposure was comparable to that described in literature in NHKs and HaCaT cells (Chen et al., 2021; Hseu et al., 2019, 2020). Repetitive UVA irradiation further increased α-MSH and EDN1 mRNA and protein expression and induced those of SCF and b-FGF (Figures 1C and 1D). The parallel irradiation of cells with UVA at the doses of 2 and 8 J/cm<sup>2</sup> reproduced the same effects on morphology and cell number reduction (20 ± 6% and 45 ± 5% reduction vs Ctr for 2 J/cm<sup>2</sup> and 8 J/cm<sup>2</sup>, respectively) and indicated the 5 J/cm<sup>2</sup> dose as the most effective in inducing the production of melanogenic factors, without showing any additional effect at 8 J/cm<sup>2</sup> (Figure S1).

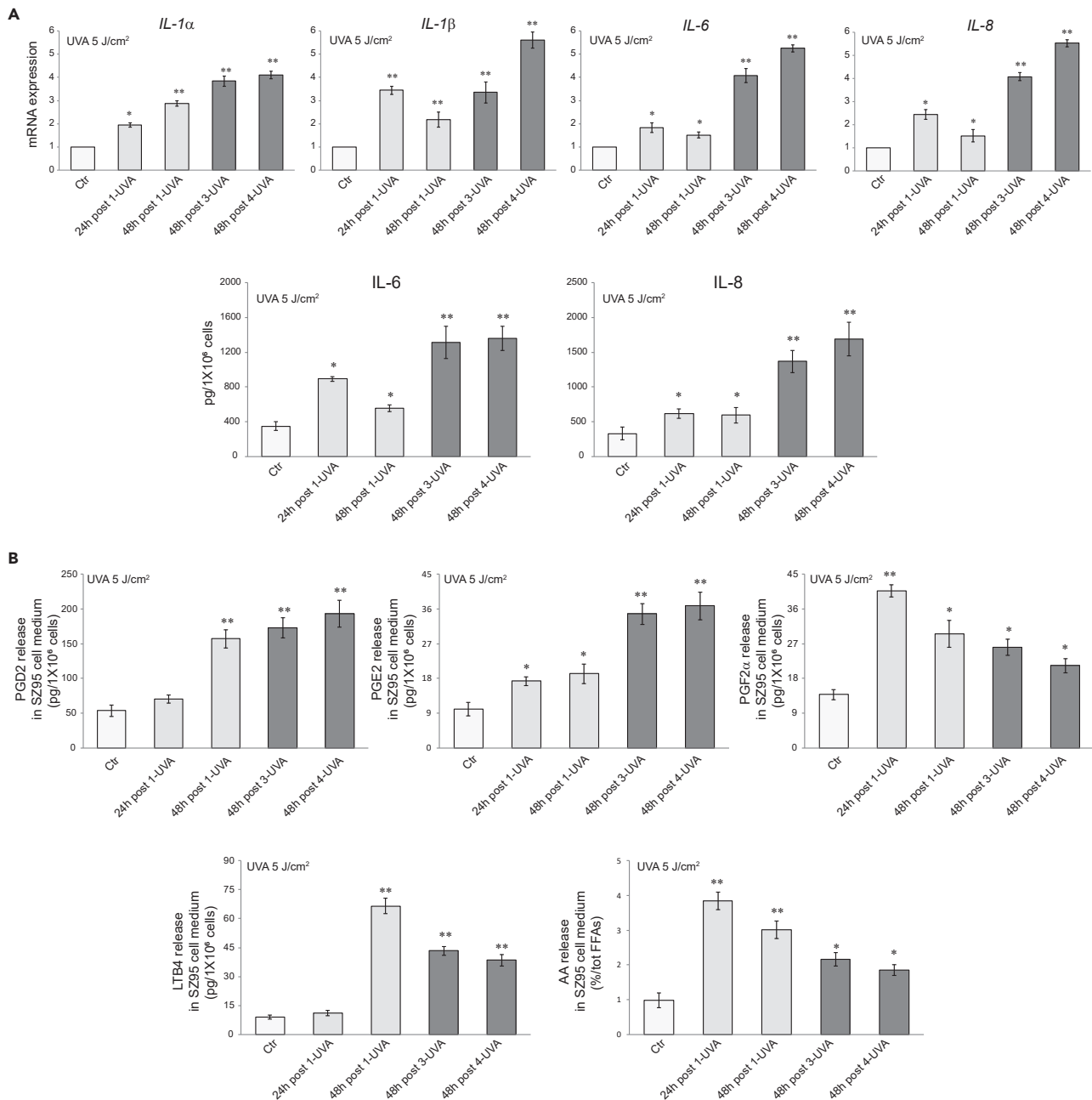
To evaluate whether the production was enduring, repeatedly irradiated (5 J/cm<sup>2</sup> for 7 times) SZ95 cells medium was collected 72 h and one week after last treatment. Significant mRNA and protein levels of the pro-melanogenic factors, and in particular of α-MSH, and EDN1, were detected, demonstrating the secretion persistence (Figure 1E).

Inflammatory cytokines have an active role in stimulating pigmentation (Cardinali et al., 2012; Kaufman et al., 2018; Okazaki et al., 2005; Rodriguez-Arambula et al., 2015). UVA irradiation significantly up-modulated the mRNA and protein expression of IL-1α, IL-1β, IL-6, and IL-8, particularly following the repetitive exposure (Figure 2A) and induced the release of lipid mediators, such as arachidonic acid, LTB4, and prostaglandins (in particular PGD2, PGE2, and PGF-2α), involved in inflammation, pigmentation, and aging process as SASP factors (Gruber et al., 2021; Kohli et al., 2021; Tomita et al., 1992) (Figure 2B). As for the growth factors, the dose of 8 J/cm<sup>2</sup> had no additional effects on the production of inflammatory mediators (Figures S2A and S2B). Following the repetitive UVA exposure, a slight induction of lipogenesis enzymes mRNA expression was observed without an effective increase of cell lipid amount (data not shown). The exposure to LPS, a notable pro-inflammatory stimulus through Toll-like receptor (TLR) binding (Nagy et al., 2006), up-modulated the mRNA and protein expression of α-MSH, EDN1, SCF, and bFGF. On the contrary, the treatment with insulin, an inducer of sebocyte metabolic pathways (Mastrofrancesco et al., 2017; Ottaviani et al., 2020) did not modify the mRNA and protein



**Figure 1. Effect of UVA irradiation on growth factors release in SZ95 sebocytes**

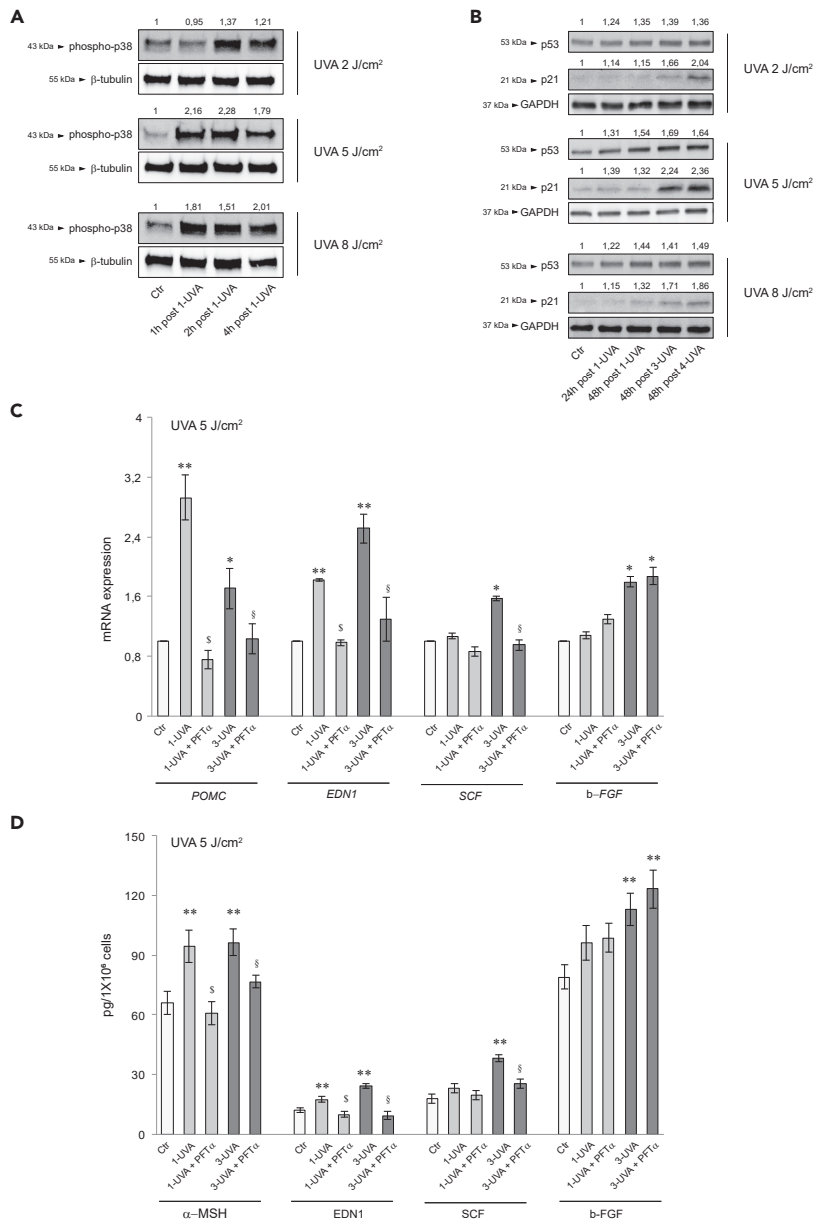
- (A) Experimental scheme of UVA irradiation of SZ95 sebocytes.
- (B) Phase-contrast analysis of SZ95 sebocytes after 4-UVA 5 J/cm<sup>2</sup> irradiations.
- (C) The mRNA expression levels of POMC, EDN1, SCF, and b-FGF in SZ95 sebocytes after 24 and 48h post 1-UVA and 48h post three or 4-UVA 5 J/cm<sup>2</sup> irradiations. Results are presented as the mean ± SD of three independent experiments and are expressed as the fold change respect to untreated control cells (\*p < 0.05, \*\*p < 0.01).
- (D) Protein quantitation by ELISA of α-MSH, EDN1, SCF, and b-FGF in SZ95 sebocytes after 24 and 48h post 1-UVA and 48h post three or 4-UVA 5 J/cm<sup>2</sup> irradiations. Results are presented as the mean ± SD of three independent experiments and are expressed in absolute quantities (\*p < 0.05, \*\*p < 0.01 vs Ctr).
- (E) The mRNA expression levels and protein quantitation by ELISA of POMC/α-MSH, EDN1, SCF, and b-FGF in SZ95 sebocytes after 72h or 1 week post 7-UVA 5 J/cm<sup>2</sup> irradiations. Data represent the mean ± SD of three independent experiments. For mRNA levels, results are expressed as the fold change respect to untreated control cells (\*\*p < 0.01). For ELISA assay, results are expressed in the absolute quantities (\*\*p < 0.01 vs Ctr).



**Figure 2. Effect of UVA irradiation on inflammatory mediators release in SZ95 sebocytes**

(A) The mRNA expression levels of *IL-1 $\alpha$* , *IL-1 $\beta$* , *IL-6*, *IL-8*, and protein quantitation by ELISA of *IL-6* and *IL-8* in SZ95 sebocytes after 24 and 48h post 1-UVA and 48h post three or 4-UVA 5 J/cm<sup>2</sup> irradiations. For mRNA levels, results are expressed as the fold change respect to untreated control cells (\*p < 0.05, \*\*p < 0.01). For ELISA assay, results are expressed in absolute quantities (\*p < 0.05, \*\*p < 0.01 vs Ctr).

(B) PGD2, PGE2, PGF2 $\alpha$ , LTB4, and AA quantitation by HPLC-MS/MS in SZ95 sebocytes after 24 and 48h post 1-UVA and 48h post three or 4-UVA 5 J/cm<sup>2</sup> irradiations. Results are expressed in absolute quantities (\*p < 0.05, \*\*p < 0.01 vs Ctr). Data represent the mean  $\pm$  SD of three independent experiments.

**Figure 3. Effect of UVA irradiation on p38MAP kinase and p53 signaling in SZ95 sebocytes**

(A) Western blot analysis of phospho-p38 protein expression in SZ95 sebocytes after 1-2-4h post irradiation with UVA 2-5-8 J/cm<sup>2</sup>. β-tubulin was used as an equal loading control. Representative blots are shown. Densitometric scanning of band intensities was performed to quantify the change of protein expression (control value taken as 1-fold in each case).

(B) Western blot analysis of p53 and p21 protein expression in SZ95 sebocytes after 24 and 48h post 1-UVA and 48h post three or 4-UVA 2-5-8 J/cm<sup>2</sup>. GAPDH was used as an equal loading control. Representative blots are shown. Densitometric scanning of band intensities was performed to quantify the change of protein expression (control value taken as 1-fold in each case).

(C) The mRNA expression levels of POMC, EDN1, SCF, and b-FGF in SZ95 sebocytes after 48h of treatment with PFTα 5 μM and one or 3-UVA 5 J/cm<sup>2</sup> irradiations. Results are presented as the mean ± SD of three independent experiments and are expressed as the fold change respect to untreated control cells (\*p < 0.05, \*\*p < 0.01 vs Ctr; \$p < 0.05 vs 1-UVA irradiated cells; §p < 0.05 vs 3-UVA irradiated cells).

(D) Protein quantitation by ELISA of αMSH, EDN1, SCF, and b-FGF in SZ95 sebocytes after 48h of treatment with PFTα 5 μM and one or 3-UVA 5 J/cm<sup>2</sup> irradiations. Results are presented as the mean ± SD of three independent experiments and are expressed in absolute quantities (\*\*p < 0.01 vs Ctr; \$p < 0.05 vs 1-UVA irradiated cells; §p < 0.05 vs 3-UVA irradiated cells).

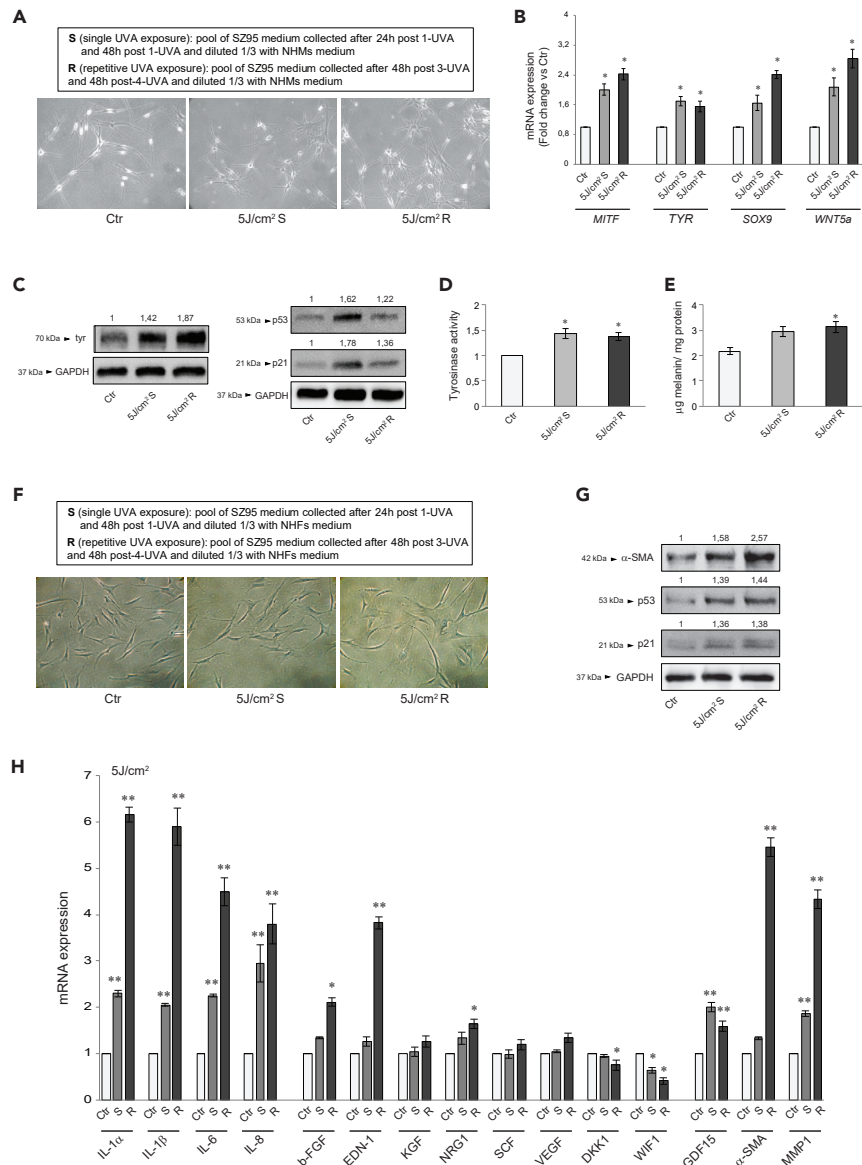
levels of the pro-melanogenic factors (Figures S3A and S3B). UVA exposure also promoted the rapid phosphorylation of the p38 MAP kinase (Figure 3A), a stressor susceptible kinase (Corre et al., 2004; Freund et al., 2011; Gu et al., 2014; Schalka 2017). Moreover, the protein expression of p53, a key player in the UV-response in keratinocytes for inducing skin pigmentation, and its downstream effector p21, were gradually upregulated (Figure 3B) (Murase et al., 2009; Choi et al., 2018; Cui et al., 2007). Specific inhibition of p53 by PFT $\alpha$  (Bellei et al., 2013; Cai et al., 2012; Luo et al., 2014a) counteracted the single or repetitive UVA-mediated induction of  $\alpha$ -MSH, EDN1, and SCF. Only the b-FGF level was not affected by p53 inhibition (Figures 3C and 3D).

Melasma occurs in childbearing age when, after puberty, SGs underwent enlargement and differentiation. Considering that SZ95 sebocytes at diverse differentiation grades display differences in metabolic pathways activation (Ottaviani et al., 2020), we evaluated the secretion pattern in early differentiated UVA irradiated SZ95 cells (SZ95-SF). In these cells, 5 J/cm<sup>2</sup> UVA exposure induced a low level of pro-inflammatory cytokines (Figure S4A) but not the evaluated pro-melanogenic factors (Figure S4B).

### Conditioned medium from irradiated SZ95 sebocytes induced melanogenesis in NHMs and a senescent phenotype in NHFs

We treated NHMs with the conditioned medium obtained from SZ95 sebocytes irradiated with 5 J/cm<sup>2</sup> UVA. NHMs incubated with sham-irradiated SZ95 cells conditioned medium retained their bipolar spindle-like morphology. Supernatant from irradiated SZ95 cells (according to the scheme in Figure 1A and the legend in Figure 4A) induced cellular flattening with increased surface area, and dendrite formation (Figure 4A), associated with the upregulation of the mRNA levels of genes involved in the melanogenesis, as the transcription factor MITF (Cheli et al., 2010; Vachtenheim and Borovansky 2010), the rate-limiting enzyme TYR (Brenner and Hearing 2008), as well as that of SOX9, and WNT5a, both implicated in melanocyte differentiation and melanogenesis (Barker 2008; Passeron et al., 2007; Rabbani et al., 2011; Sun et al., 2018; Vibert et al., 2017; Wang et al., 2015) (Figure 4B). Consistently, tyrosinase, p53, and p21 protein were markedly induced (Figure 4C), and tyrosinase activity (Figure 4D) and intracellular melanin content (Figure 4E) were significantly augmented. The effect size was comparable to that previously observed treating NHMs with Forskolin, an adenylate cyclase activator generally employed to stimulate melanogenesis (Flori et al., 2011).

Because fibroblasts secrete growth factors contributing to the paracrine signaling network controlling melanocyte function (Kapoor et al., 2020; Wang et al., 2017; Bastonini et al., 2016), we treated NHFs with the irradiated SZ95 cells conditioned medium (according to the scheme in Figure 1A and the legend in Figure 4F). NHFs incubated with sham-irradiated SZ95 sebocyte medium retained their bipolar spindle-like morphology, whereas the addition of supernatant from irradiated SZ95 cells resulted in cellular flattening and enlarged shape, features resembling a senescent phenotype (Figure 4F). Moreover, we observed a marked increase in the p53 and p21 protein expression and the direct transcriptional p53 target  $\alpha$ -SMA protein (Comer et al., 1998), expressed by photo-aged fibroblasts (Figure 4G). Then we analyzed (i) the inflammatory cytokines IL-1 $\alpha$ , IL-1 $\beta$ , IL-6, IL-8, (ii) the growth factors b-FGF, EDN-1, KGF, NRG1, SCF, VEGF, all up-modulated in stress-induced senescent fibroblasts and capable of regulating melanocyte growth, differentiation, and pigmentation (Kovacs et al., 2010; Waldera Lupa et al., 2015), and (iii) GDF15,  $\alpha$ -SMA, and MMP1, markers of photo-aged fibroblasts (Huang et al., 2019; Kim et al., 2020; Kovacs et al., 2018) (Figure 4H). Incubation with conditioned medium from single or repetitive irradiated SZ95 sebocytes upregulated the expression of all tested cytokines and the senescence markers GDF15 and MMP1. The b-FGF, EDN-1, NRG1, and  $\alpha$ -SMA transcripts were significantly induced only in fibroblasts exposed to repeated irradiated SZ95 cell supernatant, in association with a reduction of WIF1, whose downregulation stimulates tyrosinase expression (Kim et al., 2013) and DKK1, an inhibitor of melanocyte proliferation and pigmentation (Yamaguchi et al., 2007). KGF, VEGF, and SCF transcripts showed no difference. To verify whether sebocyte-specific lipids could contribute to the observed changes in NHMs and NHFs, we used lipid depleted irradiated SZ95 conditioned medium to treat these cells. No significant difference in the modulation of transcripts for pro-melanogenic factors (Figure S5A), as well as for tyrosinase activity (Figure S5B) was observed in NHMs. The same applies for pro-inflammatory cytokines, growth factors, and markers of photo-aged fibroblasts in NHFs (Figure S5C).

**Figure 4. Influences of irradiated SZ95 conditioned medium on NHMs melanogenesis and NHFs phenotype**(A) Experimental SZ95 pool medium description and phase-contrast analysis of NHMs treated with S or R UVA 5 J/cm<sup>2</sup> for 5 days.(B) The mRNA expression levels of MITF, TYR, SOX9, and WNT5a in NHMs after addition with S or R UVA 5 J/cm<sup>2</sup> for 48h. Results are presented as the mean ± SD of three independent experiments and are expressed as the fold change respect to untreated control cells (\*p < 0.05 vs Ctr).(C) Western blot analysis of tyr, p53, and p21 protein expression in NHMs after addition with S or R UVA 5 J/cm<sup>2</sup> for 72h. GAPDH was used as an equal loading control. Representative blots are shown. Densitometric scanning of band intensities was performed to quantify the change of protein expression (control value taken as 1-fold in each case).(D) Analysis of tyrosinase activity on NHMs after addition with S or R UVA 5 J/cm<sup>2</sup> for 4 days. Results are presented as the mean ± SD of three independent experiments and are expressed as the fold change respect to untreated control cells (\*p < 0.05).(E) Melanin content evaluation in NHMs after addition with S or R UVA 5 J/cm<sup>2</sup> for 5 days. Results are presented as the mean ± SD of three independent experiments and are expressed as ratio of μg melanin/mg protein (\*p < 0.05 versus Ctr).(F) Experimental SZ95 pool medium description and phase-contrast analysis of NHFs added with S or R UVA 5 J/cm<sup>2</sup> for 4 days.(G) Western blot analysis of α-SMA, p53, and p21 protein expression in NHFs after addition with S or R UVA 5 J/cm<sup>2</sup> for 4 days. GAPDH was used as an equal loading control. Representative blots are shown. Densitometric scanning of band intensities was performed to quantify the change of protein expression (control value taken as 1-fold in each case).(H) The mRNA expression levels of IL-1α, IL-1β, IL-6, IL-8, b-FGF, EDN1, KGF, NRG1, SCF, VEGF, DKK1, WIF1, GDF15, α-SMA, and MMP1 in NHFs after addition with S or R UVA 5 J/cm<sup>2</sup> for 48h. Results are presented as the mean ± SD of three independent experiments and are expressed as the fold change respect to untreated control cells (\*p < 0.05, \*\*p < 0.01 vs Ctr).

**Table 1. Treatment of NHMs**

β-Estr 1 nM	NHMs treated with β-Estradiol 1 nM
β-Estr 10 nM	NHMs treated with β-Estradiol 10 nM
R	NHMs exposed to SZ95 R
β-Estr 1 nM + R	NHMs pretreated for 24h with β-Estradiol 1 nM and then exposed to β-Estradiol 1 nM in the presence of SZ95 R
β-Estr 10 nM + R	NHMs pretreated for 24h with β-Estradiol 10 nM and then exposed to β-Estradiol 10 nM in the presence of SZ95 R

### Effects of estrogen on the dermal compartment and indirect effect on epidermal pigmentation

*Estrogen did not potentiate the UVA-induced production of pro-melanogenic factors and pro-inflammatory cytokines in SZ95 sebocytes*

The association of melasma with pregnancy or hormonal therapy usage suggests that female sex hormones, in particular estrogens, facilitate the development of the disorder (Cario 2019; Ortonne et al., 2009; Lee 2015). Because SZ95 sebocytes express estrogen receptors (ERs) (Makrantonaki et al., 2006, 2008), SZ95 cells were exposed to 1 μM 17β-estradiol (Makrantonaki et al., 2008) and then irradiated with UVA (according to the scheme in Figure S6A) to decipher the influence of estrogens on the sebocytes production of pro-melanogenic factors and pro-inflammatory cytokines. Treatment with 17β-estradiol did not potentiate the upregulation of p53 and p21 following single or repeated UVA exposure (Figure S6B). Consistently, no significant difference in the UVA-modulation of transcripts for pro-inflammatory cytokines and pro-melanogenic factors (Figure S6C), as well as for the α-MSH, EDN-1, SCF, and b-FGF protein expression (Figure S6D), was observed.

### Combined effects of β-estradiol and exposure to SZ95 conditioned medium on NHMs melanogenesis

Exposure of melanocytes to 17β-estradiol at physiological or pregnancy concentrations stimulated melanogenesis (McLeod et al., 1994; Natale et al., 2016; Ranson et al., 1988). We then evaluated whether the concurrent exposure to 17β-estradiol and the conditioned medium from repetitively irradiated SZ95 cells strengthened the melanogenic process in NHMs (see Table 1 in methods details). Individually, the stimuli induced a significant increase in tyrosinase protein expression (Figure S7A), activity (Figure S7B), and melanin content (Figure S7C), but the combined treatment was not synergistic at both doses of 17β-estradiol (Figure S7A, S7B, and S7C).

### Synergistic effect of UVA irradiation, 17β-estradiol treatment, and exposure to SZ95 conditioned medium on NHFs

NHFs, which express ERs at the mRNA and protein level (Haczynski et al., 2002), were nonirradiated or irradiated with UVA and simultaneously exposed to 1 nM 17β-estradiol plus or minus the conditioned medium from repeatedly irradiated SZ95 cells (see the scheme in Figure 5 and Table 2 in methods details), at a dilution higher (R 1/4) than that previously used (R 1/3), to reproduce a suitable *in vivo* situation. Except for a slight modulation of EDN1, GDF15, and WIF1, the R 1/4 dilution of the SZ95 cell-conditioned medium did not cause any significant change in the transcripts for pro-melanogenic factors and senescence markers (Figure 5). UVA alone only modified NRG1, WIF1, GDF15, and MMP1 transcripts, whereas 17β-estradiol alone did not significantly modulate the analyzed gene expression. Interestingly, only the simultaneous presence of all stimuli (UVA irradiation, 17β-estradiol treatment, and exposure to SZ95 cell-conditioned medium) potentiated the mRNA expression of the growth factors b-FGF, EDN1, KGF, VEGF, and NRG1, and the pro-inflammatory cytokines IL-6, IL-8, IL-1α, and IL-1β. However, the presence of 17β-estradiol did not further increase the expression of the aging markers α-SMA and MMP1 induced by the combination UVA plus UVA-irradiated SZ95 cells supernatant. Similar results were obtained with 17β-estradiol at the dose of 10 nM (Data not shown).

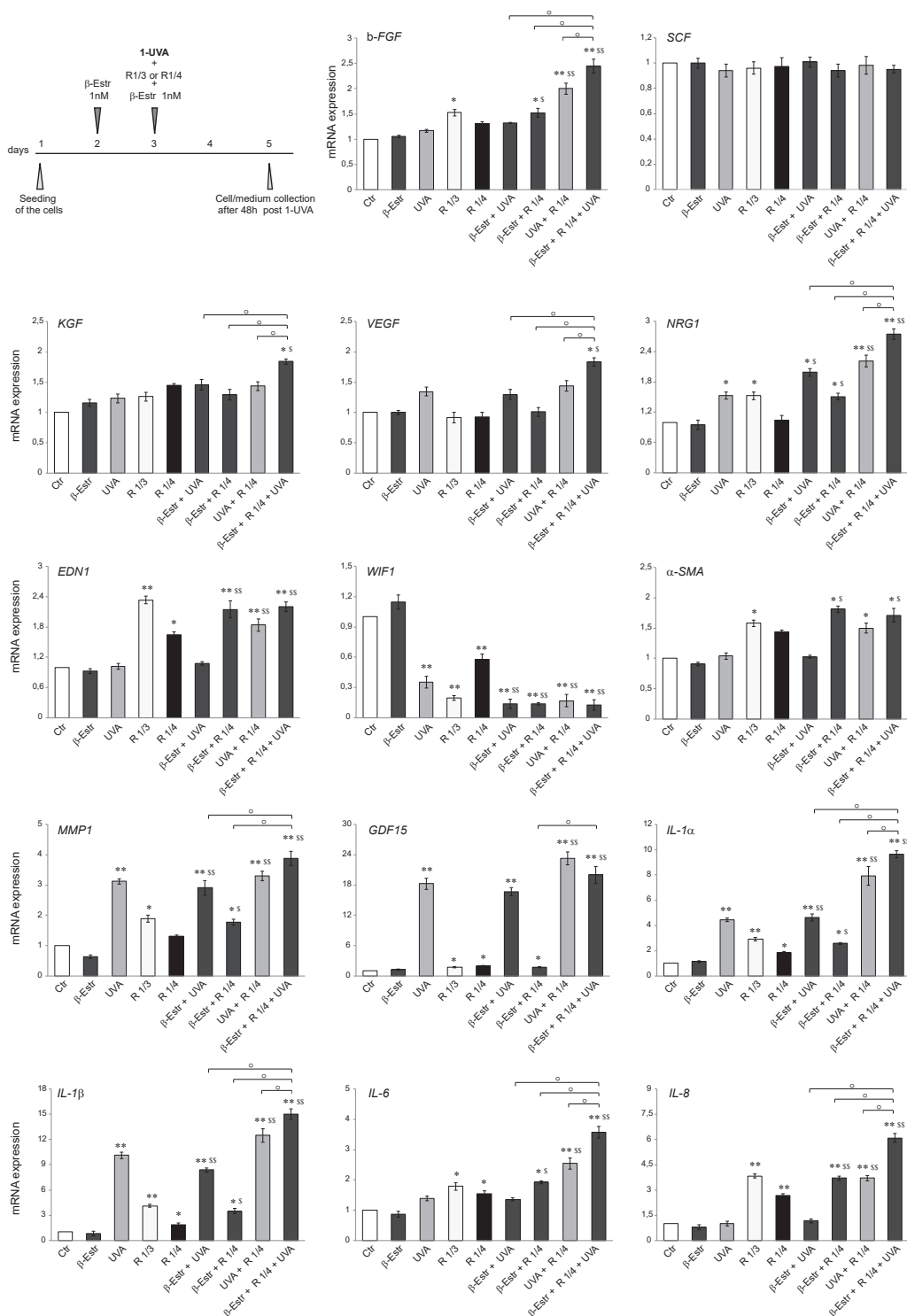


**Figure 5. Synergistic effect of UVA irradiation, 17 $\beta$ -estradiol treatment, and exposure to SZ95 conditioned medium on NHFs. Experimental scheme of 1 nM  $\beta$ -estradiol treatment, exposure to SZ95 conditioned medium, and UVA irradiation of NHFs (see Table 2 for treatments)**

The mRNA expression levels of b-FGF, SCF, KGF, VEGF, NRG1, EDN1, WIF1,  $\alpha$ -SMA, MMP1, GDF15, IL-1 $\alpha$ , IL-1 $\beta$ , L-6, and IL-8 in NHFs after treatments. Results are presented as the mean  $\pm$  SD of three independent experiments and are expressed as the fold change respect to untreated control cells (\*p < 0.05, \*\*p < 0.01 vs Ctr; \$p < 0.05, \$\$p < 0.01 vs R 1/4; °p < 0.05 vs other treatments).

**Table 2. Treatment of NHFs**

β-Estr 1 nM	NHFs treated with β-Estradiol 1 nM
UVA	NHFs irradiated with UVA 5J/cm <sup>2</sup>
R 1/3	NHFs exposed to SZ95 R; 1/3 dilution
R 1/4	NHFs exposed to SZ95 R; 1/4 dilution
β-Estr 1 nM + UVA	NHFs pretreated for 24h with β-Estradiol 1 nM, then irradiated with UVA 5J/cm <sup>2</sup> and exposed to β-Estradiol 1 nM
β-Estr 1 nM + R	NHFs treated with β-Estradiol 1 nM in the presence of SZ95 R; 1/4 dilution
UVA + R	NHFs irradiated with UVA 5J/cm <sup>2</sup> and then exposed to SZ95 R; 1/4 dilution
β-Estr 1 nM + UVA + R	NHFs pretreated for 24h with β-Estradiol 1 nM, then irradiated with UVA 5J/cm <sup>2</sup> and exposed to β-Estradiol 1 nM in the presence of SZ95 R; 1/4 dilution

### Effects of NHFs conditioned medium on NHMs melanogenesis

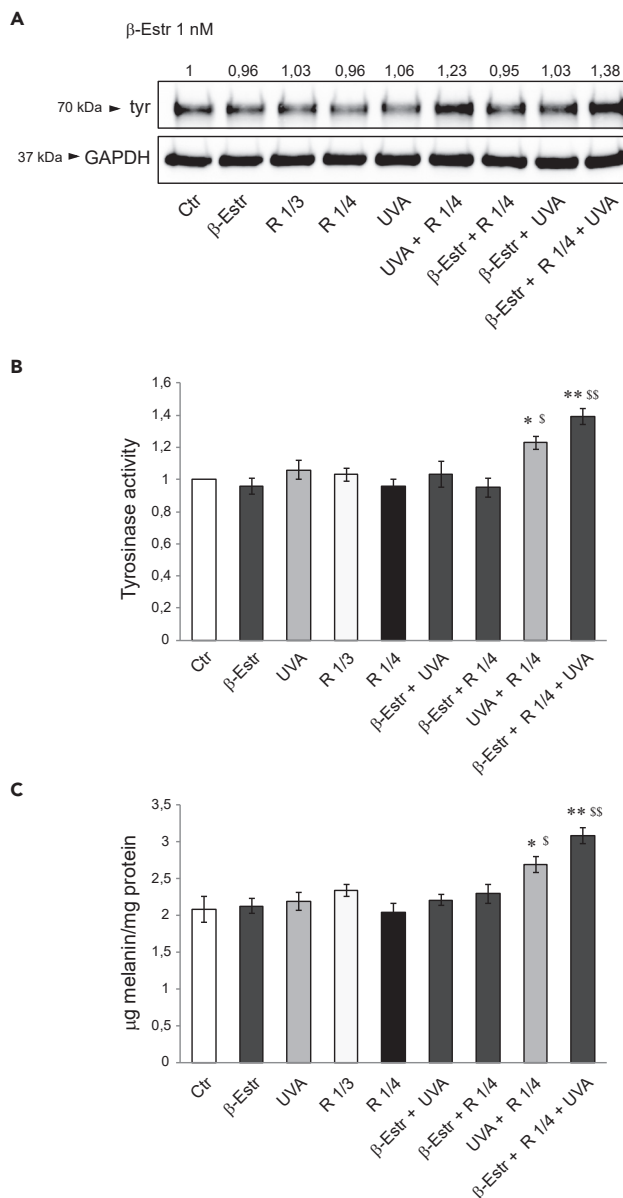
NHMs exposed to the supernatant from UVA + R NHFs, and even more to those from 17 $\beta$ -estradiol + R + UVA NHFs, significantly increased tyrosinase protein expression (Figure 6A), activity (Figure 6B), and melanin content (Figure 6C), demonstrating the synergistic activity of the entire combination resembling the *in vivo* conditions (See Table 3 in methods details).

### Melanogenesis promotion and growth factors induction in ex vivo and *in vivo* systems

To demonstrate the *in vivo* relevance of the *in vitro* results, we evaluated the pigmentation produced in human skin explants (i) maintained in coculture with SZ95 sebocytes repetitively exposed to UVA (5 J/cm<sup>2</sup>) (Figure 7A) or (ii) stimulated with a conditioned medium of irradiated SZ95 (Figure 7B). In both ex vivo models, macroscopic pigmentation was visualized (Figures 7A and 7B), because of a significant increase of melanin pigment at the basal epidermal layer and a translocation into suprabasal keratinocytes (Figures 7C and 7D) as evidenced by Fontana-Masson staining. In addition, an increased SCF expression in the cytoplasm of keratinocytes throughout all epidermal layers was observed (Figures 7E and 7F). Furthermore, SCF expression was investigated at the level of the sebaceous glands in human skin explants non-stimulated or stimulated with conditioned medium from irradiated SZ95 sebocytes. In samples stimulated with control SZ95 medium, SCF was detected in the cytoplasm of basal and early differentiated sebocytes. The stimulation with conditioned medium from irradiated sebocytes resulted in a greater SCF expression throughout the maturation zone even in the advanced differentiated cells toward the center of the gland. To further confirm the *in vitro* findings, we collected the sebum from the lesional (L) and non-lesional (NL) areas of 10 female patients with melasma. Sebum is a holocrine secretion, and sebocytes accumulate lipids during their differentiation process and then release the entire cell content in the gland ducts reaching the skin surface. Therefore, the protein content analysis allows identifying products of cell activity (Clayton et al., 2020; Ottaviani et al., 2020; Schneider and Paus 2010). Sebum collected from the L areas contained a significantly higher level of p53 protein and an increased amount of α-MSH, EDN-1, SCF, and b-FGF compared to NL skin of the same patient (Figures 7G and 7H).

## DISCUSSION

We demonstrated that sebocytes have the capability to produce several growth factors following different types of stimuli participating in the skin cells cross-talk relevant in the physiological homeostasis and pathological processes. Following UVA radiation, sebocytes, like keratinocytes (Szollosi et al., 2018), produce and upregulate the pro-melanogenic factors α-MSH, EDN1, and the stromal sustaining factors SCF and b-FGF, in addition to cytokines and lipid-derived mediators. Environmental stressors, including UV, activate the intracellular p38 MAPK pathway in the different skin cells, mediating an inflammatory response via the production of cyclooxygenase byproducts and pro-inflammatory cytokines (Chen et al., 2001; Kim et al., 2005) and sebocytes appear to be one of the targets of UVA-induced stress. In melasma dermis, p38 MAPK positive cells are present, demonstrating the pro-inflammatory role of UV in initiating the pathology (Esposito et al., 2018). UVA irradiation

**Figure 6. Effects of NHFs conditioned medium on NHMs melanogenesis**

(A) Western blot analysis of tyrosinase protein expression in NHMs after treatments with NHFs medium (see Table 3 for treatments). GAPDH was used as an equal loading control. Representative blots are shown. Densitometric scanning of band intensities was performed to quantify the change of protein expression (control value taken as 1-fold in each case).

(B) Analysis of tyrosinase activity on NHMs after treatments. Results are presented as the mean  $\pm$  SD of three independent experiments and are expressed as the fold change respect to untreated control cells (\* $p < 0.05$ , \*\* $p < 0.01$  and R 1/4 ( $\$p < 0.05$ ,  $\$\$p < 0.01$ ), respectively.

(C) Melanin content evaluation in NHMs after treatments. Results are presented as the mean  $\pm$  SD of three independent experiments and are expressed as ratio of  $\mu\text{g melanin/mg protein}$  (\* $p < 0.05$ , \*\* $p < 0.01$  versus Ctr;  $\$p < 0.05$ ,  $\$\$p < 0.01$  versus R 1/4).

significantly activated p38 MAPK in SZ95 cells and subsequently the release of the pro-inflammatory cytokines IL-1 $\alpha$  and IL-6, arachidonic acid, and the epilipidome product PGD2 and LTB4, all components of the SASP. Like in keratinocytes (Murase et al., 2009), the UVA-induced p53 expression can

**Table 3. Treatment of NHMs**

β-Estr 1 nM	NHMs treated with NHFs β-Estr 1 nM medium
UVA	NHMs treated with NHFs UVA medium
R 1/3	NHMs treated with NHFs R 1/3 medium
R 1/4	NHMs treated with NHFs R 1/4 medium
β-Estr 1 nM + UVA	NHMs treated with NHFs β-Estr 1 nM + UVA medium
β-Estr 1 nM + R	NHMs treated with NHFs β-Estr 1 nM + R medium
UVA + R	NHMs treated with NHFs UVA + R medium
β-Estr 1 nM + UVA + R	NHMs treated with NHFs β-Estr 1 nM + UVA + R medium

explain the growth factor gene activation, as confirmed by its pharmacological inhibition. Repetitive exposures further increased the production even at least for 48 h after the last irradiation, showing the contribution of sebocytes in driving modifications of fibroblast and melanocyte behavior through an inflamming process, even after the suspension of solar exposure (Gruber et al., 2021; Franceschi and Campisi 2014; Jinlian et al., 2007; Muthusamy and Piva 2013; Narzt et al., 2021). SZ95 cells cannot be considered a suitable model to evaluate the photo-aging process being an established cell line. However, repeated UVA irradiations displayed a progressive and irregular cell enlargement and a reduction of proliferative rate, showing features of cell differentiation and aging in correlation with the induction of pro-melanogenic mediators.

LPS exposure of SZ95 cells led to a similar production of growth factors, whereas insulin treatment did not induce the secretion of any of the analyzed growth factors. Moreover, UVA radiation did not influence the sebum composition of SZ95 cells and the treatment with lipid depleted SZ95 supernatants did not modify the observed effects on NHMs and NHFs, indicating that growth factors and SGs lipid production are two processes following different pathways and that the growth factors release represents a stress response to several stimuli.

Skin explants cocultures with SZ95 sebocytes strengthened the role of these cells in the melanogenesis promotion through the secretion of growth factors by dermal cells. The increased melanin content was associated with a strong expression of SCF, a key factor in skin hyperpigmented disorders (Atef et al., 2019). Furthermore, the presence of SZ95 sebocytes in the cocultures resulted in the overall improved structural integrity of the epidermis, as previously demonstrated (Nikolakis et al., 2015). Thus, the ex vivo models provide evidence that the bioactive molecules released by sebocytes following pro-inflammatory stimuli such as UVA contribute to promoting skin homeostasis and pigmentation that could be relevant in several other physiological and pathological conditions such as post-acne hyperpigmentation and wound healing. Interestingly, our ex vivo data demonstrated a basal production of growth factors, in particular of SCF, in early differentiated sebocytes of sebaceous glands. The stimulation with conditioned medium of irradiated SZ95 cells induced the SCF increase in the late differentiated sebocytes responsible for the sebum production and release on the skin surface. Because we previously demonstrated that the proteins present in the sebum are mainly produced by sebocytes (Ottaviani et al., 2020), the higher content of p53 and melanogenic growth factors determined in sebum from lesional areas with respect to non-lesional ones highlighted the active role of sebaceous glands in the complex cell-cell network regulating skin pigmentation.

Melasma shows features of sun-damaged skin, and the different factors secreted by photo-aged fibroblasts might have a crucial role in its physiopathology (Kwon et al., 2019; Passeron and Picardo 2018; Kapoor et al., 2020; Kim et al., 2013, 2019; Kang et al., 2010). Fibroblasts isolated from photo-aged skin or with an *in vitro* UV-induced senescence-like phenotype, produce a significant amount of cytokines and pro-melanogenic factors, such as KGF, HGF, SCF, and GDF15 (Kim et al., 2020; Briganti et al., 2013; Duval et al., 2014), which are overexpressed in lesional melasma skin (Byun et al., 2016; Chen et al., 2010; Hasegawa et al., 2015; Kang et al., 2006). On the contrary, the inhibitor factor WIF-1, whose downregulation in fibroblasts in 3D models stimulates tyrosinase expression in melanocytes and melanosome transfer in keratinocytes, was significantly reduced (Kim et al., 2013). A decrease of p16-positive fibroblasts, associated with increased procollagen-1 expression, and a significant reduction of

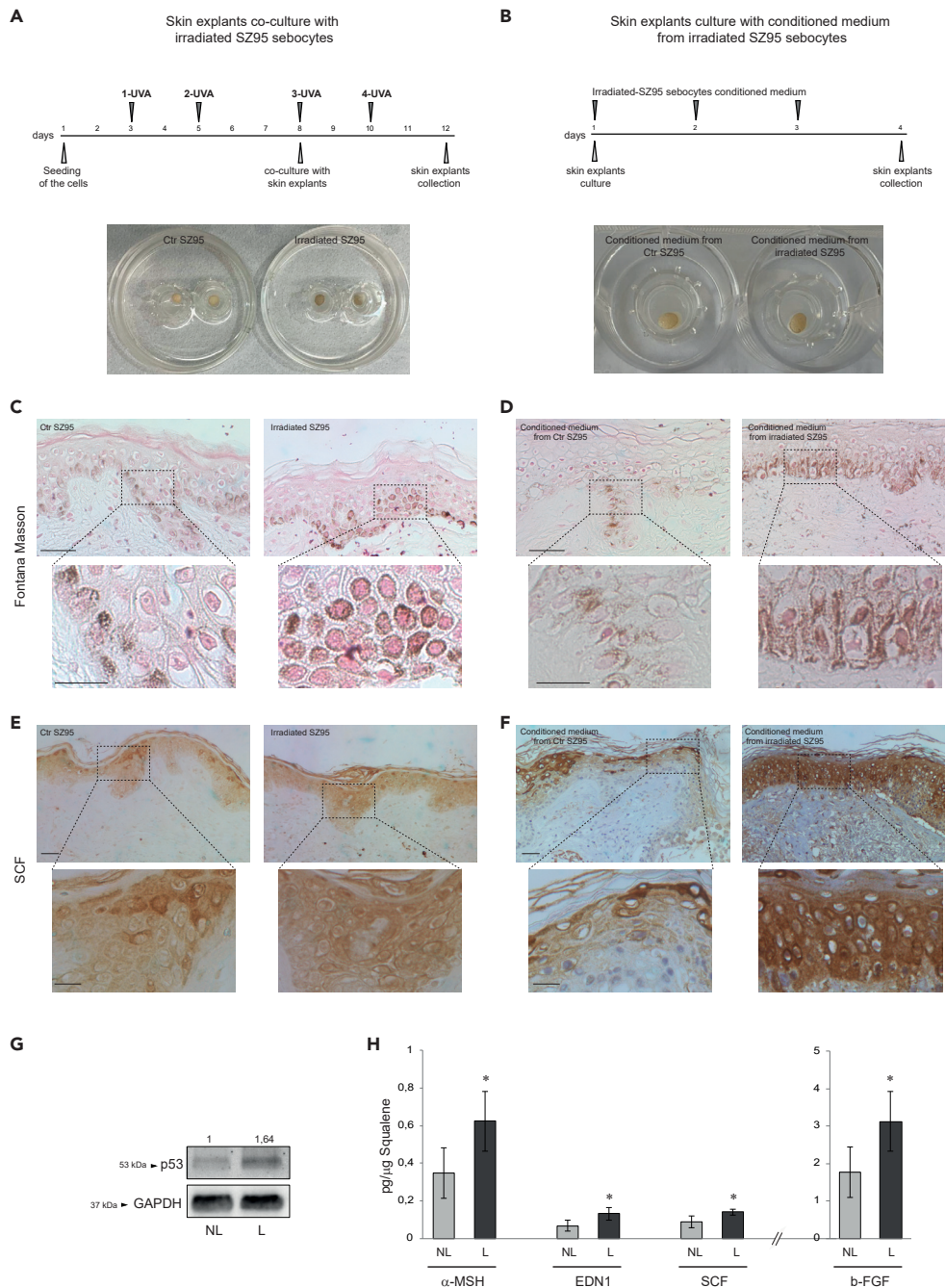


**Figure 7. Melanogenesis promotion and growth factors induction in ex vivo and in vivo systems**

- (A) Experimental schemes and macroscopic visualization of ex vivo skin explants coculture with UVA irradiated SZ95 sebocytes.
- (B) Experimental schemes and macroscopic visualization of ex vivo skin explants cultured with conditioned medium from irradiated SZ95 sebocytes.
- (C and D) Pigmentation of ex vivo skin explants visualized by Fontana-Masson staining. Scale bars: 50 and 20 μM for low and high magnification, respectively.
- (E and F) Immunohistochemical analysis of SCF expression. Scale bars: 50 and 20 μM for low and high magnification, respectively.
- (G) Immunohistochemical analysis of SCF expression in the sebaceous glands of ex vivo skin explants stimulated with conditioned medium from control and irradiated SZ95 sebocytes. Scale bars: 50 μM
- (H) Western blot analysis of p53 protein expression on sebatape from lesional (L) or non-lesional (NL) melasma skin. GAPDH was used as an equal loading control. Representative blots are shown. Densitometric scanning of band intensities was performed to quantify the change of protein expression (NL control value taken as 1-fold in each case).
- (I) Protein quantitation by ELISA of α-MSH, EDN1, SCF, and b-FGF in sebum samples. Results are presented as the mean ± SD and are expressed in absolute quantities (\*p < 0.05 vs Ctr).

epidermal pigmentation, has been obtained in radiofrequency treated melasma (Kim et al., 2019). All these data strengthen the concept that enhanced melanocyte activity in melasma is related to a senescence process involving the dermal compartment. In this context, sebocytes may exert a paracrine effect inducing an inflammasome process contributing to melanocyte proliferation, differentiation, and melanogenesis. It is noteworthy that, after repeated UVA exposure, cytokine and growth factor production from sebocytes was long-lasting, underlying the role of enduring inflammatory and photo-aged environment able to locally participate in activating hyperpigmentation even after stopping the solar exposure, thus enforcing the melanogenic activity of keratinocytes. Even if in UV-exposed skin, aside from fibroblasts and keratinocytes, other cells, such as endothelial ones, release biological factors contributing to hyperpigmentation development (Kim et al., 2007, 2018; Kang et al., 2010; Regazzetti et al., 2015), our data indicate sebocytes as one of the relevant actors in the melasma appearance explaining the peculiar localization on the face.

The preferential development during women' reproductive lifespan and the association with oral contraceptives and pregnancy indicate female sex hormones, especially estrogens, as relevant in the development and aggravation of the disorder (Ortonne et al., 2009; Lee 2015; Muallem and Rubeiz 2006). However, experiments on skin explants indicated that, even at the doses observed during pregnancy, estrogens are not able to induce hyperpigmentation alone but act in synergy with other triggers such as UVB (Cario 2019; Gauthier et al., 2019). In our model, estrogens enhanced the production of melanogenic factors when used in combination with UVA and conditioned medium from irradiated SZ95 sebocytes through a synergic effect on fibroblasts without increasing the induced aging process. The local different responsiveness of fibroblasts to steroid hormones could explain the appearance of the manifestation, analogously to the areola hyperpigmentation in pregnancy (Luo et al., 2014b; Mukudai et al., 2015).

In conclusion, our data open a new view on the role of the SGs in skin homeostasis and pathologies, and indicate that SGs have a role in activating and maintaining localized dermal inflammation and aging. Fibroblasts appear to be the prevalent target of the inflammatory mediators and hormonal stimuli in the occurrence in melasma. Moreover, the study further confirms the value of the sebum protein analyses in the evaluation of sebocyte activities.

### Limitations of the study

A limitation of this study is the employment of an immortalized human SG cell line, although considered an *in vitro* reliable model to study human sebocyte physiopathological aspects (Schneider and Zouboulis 2018; Zouboulis et al., 1999). Despite the *in vivo* data confirming the *in vitro* results, the use of skin melasma biopsies would be a valuable addition but they are difficult to obtain because melasma is a disorder mainly localized on the face of young women (Afaq and Katiyar 2011).

Moreover, in the current experimental model, other dermis components, such as endothelial cells, known to release biological factors contributing to epidermal hyperpigmentation (Kim et al., 2007, 2018; Kang et al., 2010; Regazzetti et al., 2015) have not been considered. Nevertheless, this study focused on the investigation of the sebocytes' specific contribution to the particular localization of the disorder on specific face areas rich in sebaceous glands.

### STAR★METHODS

Detailed methods are provided in the online version of this paper and include the following:

- KEY RESOURCES TABLE
- RESOURCE AVAILABILITY
  - Lead contact
  - Materials availability
  - Data and code availability
- EXPERIMENTAL MODEL AND SUBJECT DETAILS
  - Cells
  - Human subjects
- METHODS DETAILS
  - UVA irradiation treatment of SZ95 sebocytes and NHFs

- Cell treatments
- Morphologic analysis by inverted phase contrast microscope
- RNA extraction and quantitative real-time PCR
- Protein determination by sandwich enzyme-linked immunosorbent assay (ELISA)
- Assessment of pro-inflammatory lipid mediators' cellular concentrations
- Western blot analysis
- Tyrosinase assay
- Melanin content determination
- Lipid depletion
- Skin explants and co-culture experiments
- Immunohistochemical analysis
- Protein and squalene extraction from sebutape
- Squalene GC-MS analysis

● QUANTIFICATION AND STATISTICAL ANALYSIS

## SUPPLEMENTAL INFORMATION

Supplemental information can be found online at <https://doi.org/10.1016/j.isci.2022.103871>.

## ACKNOWLEDGMENTS

This work was supported by public funds from the Italian Ministry of Health. Graphical abstract was created using images from Servier Medical Art Commons Attribution 3.0 Unported License (<http://smart.servier.com>).

## AUTHOR CONTRIBUTIONS

Conceptualization, E.F., A.M., and M.P.; Formal analysis, E.F., A.M., M.O., S.B., and G.C.; Funding acquisition, M.P.; Investigation, E.F., A.M., S.M., M.O., S.B., G.C., A.F., and N.C.; Methodology, E.F., A.M., M.O., S.B., G.C., and M.Z.; Supervision, C.C.Z., M.P.; Validation, E.F., A.M., S.M., M.O., S.B., and G.C.; Writing-original draft, E.F., S.M., M.O., S.B., and G.C.; Writing-review & editing, E.F., A.M., S.M., M.O., S.B., C.C.Z., and M.P.

## DECLARATION OF INTERESTS

The authors declare no competing interests

Received: September 27, 2021

Revised: December 14, 2021

Accepted: January 28, 2022

Published: March 18, 2022

## REFERENCES

- Abdel-Naser, M.B., Seltmann, H., and Zouboulis, C.C. (2012). SZ95 sebocytes induce epidermal melanocyte dendrity and proliferation in vitro. *Exp. Dermatol.* 21, 393–395.
- Afaq, F., and Katiyar, S.K. (2011). Polyphenols: skin photoprotection and inhibition of photocarcinogenesis. *Mini Rev. Med. Chem.* 11, 1200–1215.
- Atef, A., El-Rashidy, M.A., Abdel Azeem, A., and Kabel, A.M. (2019). The role of stem cell factor in hyperpigmented skin lesions. *Asian Pac. J. Cancer Prev.* 20, 3723–3728.
- Bak, H., Lee, H.J., Chang, S.E., Choi, J.H., Kim, M.N., and Kim, B.J. (2009). Increased expression of nerve growth factor receptor and neural endopeptidase in the lesional skin of melasma. *Dermatol. Surg.* 35, 1244–1250.
- Barker, N. (2008). The canonical Wnt/beta-catenin signalling pathway. *Methods Mol. Biol.* 468, 5–15.
- Bastonini, E., Kovacs, D., and Picardo, M. (2016). Skin pigmentation and pigmentary disorders: focus on epidermal/dermal cross-talk. *Ann. Dermatol.* 28, 279–289.
- Bellei, B., Pitisci, A., Ottaviani, M., Ludovici, M., Cota, C., Luzi, F., Dell'Anna, M.L., and Picardo, M. (2013). Vitiligo: a possible model of degenerative diseases. *PLoS One* 8, e59782.
- Bohm, M., Schiller, M., Stander, S., Seltmann, H., Li, Z., Brzoska, T., Metze, D., Schiöth, H.B., Skottner, A., Seiffert, K., et al. (2002). Evidence for expression of melanocortin-1 receptor in human sebocytes in vitro and in situ. *J. Invest. Dermatol.* 118, 533–539.
- Boukari, F., Jourdan, E., Fontas, E., Montaudie, H., Castela, E., Lacour, J.P., and Passeron, T. (2015). Prevention of melasma relapses with sunscreen combining protection against UV and short wavelengths of visible light: a prospective randomized comparative trial. *J. Am. Acad. Dermatol.* 72, 189–190.e1.
- Brenner, M., and Hearing, V.J. (2008). Modifying skin pigmentation - approaches through intrinsic biochemistry and exogenous agents. *Drug Discov. Today Dis. Mech.* 5, e189–e199.
- Briganti, S., Flori, E., Mastrofrancesco, A., Kovacs, D., Camera, E., Ludovici, M., Cardinali, G., and Picardo, M. (2013). Azelaic

- acid reduced senescence-like phenotype in photo-irradiated human dermal fibroblasts: possible implication of PPARgamma. *Exp. Dermatol.* 22, 41–47.
- Briganti, S., Flori, E., Bellei, B., and Picardo, M. (2014). Modulation of PPARgamma provides new insights in a stress induced premature senescence model. *PLoS One* 9, e104045.
- Byun, J.W., Park, I.S., Choi, G.S., and Shin, J. (2016). Role of fibroblast-derived factors in the pathogenesis of melasma. *Clin. Exp. Dermatol.* 41, 601–609.
- Cai, B.H., Hsu, P.C., Hsin, I.L., Chao, C.F., Lu, M.H., Lin, H.C., Chiou, S.H., Tao, P.L., and Chen, J.Y. (2012). P53 acts as a Co-repressor to regulate keratin 14 expression during epidermal cell differentiation. *PLoS One* 7, e41742.
- Camera, E., Ludovici, M., Tortorella, S., Sinagra, J.L., Capitanio, B., Goracci, L., and Picardo, M. (2016). Use of lipidomics to investigate sebum dysfunction in juvenile acne. *J. Lipid Res.* 57, 1051–1058.
- Cardinali, G., Kovacs, D., and Picardo, M. (2012). Mechanisms underlying post-inflammatory hyperpigmentation: lessons from solar lentigo. *Ann. Dermatol. Venereol.* 139 (Suppl 4), S148–S152.
- Cario, M. (2019). How hormones may modulate human skin pigmentation in melasma: an in vitro perspective. *Exp. Dermatol.* 28, 709–718.
- Cheli, Y., Ohanna, M., Ballotti, R., and Bertolotto, C. (2010). Fifteen-year quest for microphthalmia-associated transcription factor target genes. *Pigment Cell. Melanoma Res.* 23, 27–40.
- Chen, N., Hu, Y., Li, W.H., Eisinger, M., Seiberg, M., and Lin, C.B. (2010). The role of keratinocyte growth factor in melanogenesis: a possible mechanism for the initiation of solar lentigines. *Exp. Dermatol.* 19, 865–872.
- Chen, S.J., Hseu, Y.C., Gowrisankar, Y.V., Chung, Y.T., Zhang, Y.Z., Way, T.D., and Yang, H.L. (2021). The anti-melanogenic effects of 3-O-ethyl ascorbic acid via Nrf2-mediated alpha-MSH inhibition in UVA-irradiated keratinocytes and autophagy induction in melanocytes. *Free Radic. Biol. Med.* 173, 151–169.
- Chen, W., Tang, Q., Gonzales, M.S., and Bowden, G.T. (2001). Role of p38 MAP kinases and ERK in mediating ultraviolet-B induced cyclooxygenase-2 gene expression in human keratinocytes. *Oncogene* 20, 3921–3926.
- Choi, S.Y., Bin, B.H., Kim, W., Lee, E., Lee, T.R., and Cho, E.G. (2018). Exposure of human melanocytes to UVB twice and subsequent incubation leads to cellular senescence and senescence-associated pigmentation through the prolonged p53 expression. *J. Dermatol. Sci.* 90, 303–312.
- Clayton, R.W., Langan, E.A., Ansell, D.M., de Vos, I.J.H.M., Gobel, K., Schneider, M.R., Picardo, M., Lim, X., van Steensel, M.A.M., and Paus, R. (2020). Neuroendocrinology and neurobiology of sebaceous glands. *Biol. Rev. Camb. Philos. Soc.* 95, 592–624.
- Comer, K.A., Dennis, P.A., Armstrong, L., Catino, J.J., Kastan, M.B., and Kumar, C.C. (1998). Human smooth muscle alpha-actin gene is a transcriptional target of the p53 tumor suppressor protein. *Oncogene* 16, 1299–1308.
- Corre, S., Primot, A., Sviderskaya, E., Bennett, D.C., Vaulont, S., Goding, C.R., and Galibert, M.D. (2004). UV-induced expression of key component of the tanning process, the POMC and MC1R genes, is dependent on the p-38-activated upstream stimulating factor-1 (USF-1). *J. Biol. Chem.* 279, 51226–51233.
- Cui, R., Widlund, H.R., Feige, E., Lin, J.Y., Wilensky, D.L., Igras, V.E., D’Orazio, J., Fung, C.Y., Schanbacher, C.F., Granter, S.R., and Fisher, D.E. (2007). Central role of p53 in the suntan response and pathologic hyperpigmentation. *Cell* 128, 853–864.
- Del Bino, S., Duval, C., and Bernerd, F. (2018). Clinical and biological characterization of skin pigmentation diversity and its consequences on UV impact. *Int. J. Mol. Sci.* 19, 2668. <https://doi.org/10.3390/ijms19092668>.
- Duteil, L., Cardot-Leccia, N., Queille-Roussel, C., Maubert, Y., Harmelin, Y., Boukari, F., Ambrosetti, D., Lacour, J.P., and Passeron, T. (2014). Differences in visible light-induced pigmentation according to wavelengths: a clinical and histological study in comparison with UVB exposure. *Pigment Cell. Melanoma Res.* 27, 822–826.
- Duval, C., Cohen, C., Chagnoleau, C., Flouret, V., Bourreau, E., and Bernerd, F. (2014). Key regulatory role of dermal fibroblasts in pigmentation as demonstrated using a reconstructed skin model: impact of photo-aging. *PLoS One* 9, e114182.
- Esposito, A.C.C., Brianza, G., de Souza, N.P., Miot, L.D.B., Marques, M.E.A., and Miot, H.A. (2018). Exploring pathways for sustained melanogenesis in facial melasma: an immunofluorescence study. *Int. J. Cosmet. Sci.* 40, 420–424.
- Flori, E., Mastrofrancesco, A., Kovacs, D., Ramot, Y., Briganti, S., Bellei, B., Paus, R., and Picardo, M. (2011). 2,4,6-Octatrienoic acid is a novel promoter of melanogenesis and antioxidant defence in normal human melanocytes via PPAR-gamma activation. *Pigment Cell. Melanoma Res.* 24, 618–630.
- Franceschi, C., and Campisi, J. (2014). Chronic inflammation (inflammaging) and its potential contribution to age-associated diseases. *J. Gerontol. A Biol. Sci. Med. Sci.* 69 (Suppl 1), S4–S9.
- Freund, A., Patil, C.K., and Campisi, J. (2011). p38MAPK is a novel DNA damage response-independent regulator of the senescence-associated secretory phenotype. *EMBO J.* 30, 1536–1548.
- Furugen, A., Yamaguchi, H., and Mano, N. (2015). Simultaneous quantification of leukotrienes and hydroxyeicosatetraenoic acids in cell culture medium using liquid chromatography/tandem mass spectrometry. *Biomed. Chromatogr.* 29, 1084–1093.
- Gauthier, Y., Cario, M., Pain, C., Lepreux, S., Benzekri, L., and Taieb, A. (2019). Oestrogen associated with ultraviolet B irradiation recapitulates the specific melanosome distribution observed in caucasoid melasma. *Br. J. Dermatol.* 180, 951–953.
- Gruber, F., Marchetti-Deschmann, M., Kremslechner, C., and Schosserer, M. (2021). The skin epilipidome in stress, aging, and inflammation. *Front. Endocrinol.(Lausanne)* 11, 607076.
- Gu, W.J., Ma, H.J., Zhao, G., Yuan, X.Y., Zhang, P., Liu, W., Ma, L.J., and Lei, X.B. (2014). Additive effect of heat on the UVB-induced tyrosinase activation and melanogenesis via ERK/p38/MITF pathway in human epidermal melanocytes. *Arch. Dermatol. Res.* 306, 583–590.
- Haczynski, J., Tarkowski, R., Jarzabek, K., Slomczynska, M., Wolczynski, S., Magoffin, D.A., Jakowicki, J.A., and Jakimiuk, A.J. (2002). Human cultured skin fibroblasts express estrogen receptor alpha and beta. *Int. J. Mol. Med.* 10, 149–153.
- Handel, A.C., Lima, P.B., Tonolli, V.M., Miot, L.D., and Miot, H.A. (2014a). Risk factors for facial melasma in women: a case-control study. *Br. J. Dermatol.* 171, 588–594.
- Handel, A.C., Miot, L.D., and Miot, H.A. (2014b). Melasma: a clinical and epidemiological review. *An. Bras. Dermatol.* 89, 771–782.
- Hasegawa, K., Fujiwara, R., Sato, K., Shin, J., Kim, S.J., Kim, M., and Kang, H.Y. (2015). Possible involvement of keratinocyte growth factor in the persistence of hyperpigmentation in both human facial solar lentigines and melasma. *Ann. Dermatol.* 27, 626–629.
- Hernandez-Barrera, R., Torres-Alvarez, B., Castanedo-Cazares, J.P., Oros-Ovalle, C., and Moncada, B. (2008). Solar elastosis and presence of mast cells as key features in the pathogenesis of melasma. *Clin. Exp. Dermatol.* 33, 305–308.
- Hirobe, T. (2005). Role of keratinocyte-derived factors involved in regulating the proliferation and differentiation of mammalian epidermal melanocytes. *Pigment Cell Res* 18, 2–12.
- Hseu, Y.C., Ho, Y.G., Mathew, D.C., Yen, H.R., Chen, X.Z., and Yang, H.L. (2019). The in vitro and in vivo depigmenting activity of Coenzyme Q10 through the down-regulation of alpha-MSH signaling pathways and induction of Nrf2/ARE-mediated antioxidant genes in UVA-irradiated skin keratinocytes. *Biochem. Pharmacol.* 164, 299–310.

- Hseu, Y.C., Chen, X.Z., Vudhya Gowrisankar, Y., Yen, H.R., Chuang, J.Y., and Yang, H.L. (2020). The skin-whitening effects of ectoine via the suppression of alpha-MSH-stimulated melanogenesis and the activation of antioxidant Nrf2 pathways in UVA-irradiated keratinocytes. *Antioxidants (Basel)* 9, 63. <https://doi.org/10.3390/antiox9010063>.
- Huang, K.F., Ma, K.H., Chang, Y.J., Lo, L.C., Jhap, T.Y., Su, Y.H., Liu, P.S., and Chueh, S.H. (2019). Baicalein inhibits matrix metalloproteinase 1 expression via activation of TRPV1-Ca-ERK pathway in ultraviolet B-irradiated human dermal fibroblasts. *Exp. Dermatol.* 28, 568–575.
- Im, S., Kim, J., On, W.Y., and Kang, W.H. (2002). Increased expression of alpha-melanocyte-stimulating hormone in the lesional skin of melasma. *Br. J. Dermatol.* 146, 165–167.
- Imokawa, G. (2004). Autocrine and paracrine regulation of melanocytes in human skin and in pigmentary disorders. *Pigment Cell Res.* 17, 96–110.
- Jinlian, L., Yingbin, Z., and Chunbo, W. (2007). p38 MAPK in regulating cellular responses to ultraviolet radiation. *J. Biomed. Sci.* 14, 303–312.
- Kang, H.Y., Hwang, J.S., Lee, J.Y., Ahn, J.H., Kim, J.Y., Lee, E.S., and Kang, W.H. (2006). The dermal stem cell factor and c-kit are overexpressed in melasma. *Br. J. Dermatol.* 154, 1094–1099.
- Kang, H.Y., Bahadoran, P., Suzuki, I., Zugaj, D., Khemis, A., Passeron, T., Andres, P., and Ortonne, J.P. (2010). In vivo reflectance confocal microscopy detects pigmentary changes in melasma at a cellular level resolution. *Exp. Dermatol.* 19, e228–e233.
- Kang, W.H., Yoon, K.H., Lee, E.S., Kim, J., Lee, K.B., Yim, H., Sohn, S., and Im, S. (2002). Melasma: histopathological characteristics in 56 Korean patients. *Br. J. Dermatol.* 146, 228–237.
- Kapoor, R., Dhatwalia, S.K., Kumar, R., Rani, S., and Parsad, D. (2020). Emerging role of dermal compartment in skin pigmentation: comprehensive review. *J. Eur. Acad. Dermatol. Venereol.* 34, 2757–2765.
- Kaufman, B.P., Aman, T., and Alexis, A.F. (2018). Postinflammatory hyperpigmentation: epidemiology, clinical presentation, pathogenesis and treatment. *Am. J. Clin. Dermatol.* 19, 489–503.
- Kim, E.H., Kim, Y.C., Lee, E.S., and Kang, H.Y. (2007). The vascular characteristics of melasma. *J. Dermatol. Sci.* 46, 111–116.
- Kim, H., Rhee, S.H., Kokkotou, E., Na, X., Savidge, T., Moyer, M.P., Pothoulakis, C., and LaMont, J.T. (2005). Clostridium difficile toxin A regulates inducible cyclooxygenase-2 and prostaglandin E2 synthesis in colonocytes via reactive oxygen species and activation of p38 MAPK. *J. Biol. Chem.* 280, 21237–21245.
- Kim, J.Y., Lee, T.R., and Lee, A.Y. (2013). Reduced WIF-1 expression stimulates skin hyperpigmentation in patients with melasma. *J. Invest. Dermatol.* 133, 191–200.
- Kim, M., Shibata, T., Kwon, S., Park, T.J., and Kang, H.Y. (2018). Ultraviolet-irradiated endothelial cells secrete stem cell factor and induce epidermal pigmentation. *Sci. Rep.* 8, 4235.
- Kim, M., Kim, S.M., Kwon, S., Park, T.J., and Kang, H.Y. (2019). Senescent fibroblasts in melasma pathophysiology. *Exp. Dermatol.* 28, 719–722.
- Kim, Y., Kang, B., Kim, J.C., Park, T.J., and Kang, H.Y. (2020). Senescent fibroblast-derived GDF15 induces skin pigmentation. *J. Invest. Dermatol.* 140, 2478–2486.e4.
- Kohli, J., Wang, B., Brandenburg, S.M., Basisty, N., Evangelou, K., Varela-Eirin, M., Campisi, J., Schilling, B., Gorgoulis, V., and Demaria, M. (2021). Algorithmic assessment of cellular senescence in experimental and clinical specimens. *Nat. Protoc.* 16, 2471–2498.
- Kovacs, D., Cardinali, G., Aspita, N., Cota, C., Luzi, F., Bellei, B., Briganti, S., Amantea, A., Torrisi, M.R., and Picardo, M. (2010). Role of fibroblast-derived growth factors in regulating hyperpigmentation of solar lentigo. *Br. J. Dermatol.* 163, 1020–1027.
- Kovacs, D., Bastonini, E., Ottaviani, M., Cota, C., Migliano, E., Dell'Anna, M.L., and Picardo, M. (2018). Vitiligo skin: exploring the dermal compartment. *J. Invest. Dermatol.* 138, 394–404.
- Kurokawa, I., Danby, F.W., Ju, Q., Wang, X., Xiang, L.F., Xia, L., Chen, W., Nagy, I., Picardo, M., Suh, D.H., et al. (2009). New developments in our understanding of acne pathogenesis and treatment. *Exp. Dermatol.* 18, 821–832.
- Kwon, S.H., Hwang, Y.J., Lee, S.K., and Park, K.C. (2016). Heterogeneous pathology of melasma and its clinical implications. *Int. J. Mol. Sci.* 17, 824. <https://doi.org/10.3390/ijms17060824>.
- Kwon, S.H., Na, J.I., Choi, J.Y., and Park, K.C. (2019). Melasma: updates and perspectives. *Exp. Dermatol.* 28, 704–708.
- Lakhdar, H., Zouhair, K., Khadir, K., Essari, A., Richard, A., Seite, S., and Rougier, A. (2007). Evaluation of the effectiveness of a broad-spectrum sunscreen in the prevention of chloasma in pregnant women. *J. Eur. Acad. Dermatol. Venereol.* 21, 738–742.
- Lan, C.E., Hung, Y.T., Fang, A.H., and Ching-Shuang, W. (2019). Effects of irradiance on UVA-induced skin aging. *J. Dermatol. Sci.* 94, 220–228.
- Le Faouder, P., Baillif, V., Spreadbury, I., Motta, J.P., Rousset, P., Chene, G., Guigne, C., Terce, F., Vanner, S., Vergnolle, N., et al. (2013). LC-MS/MS method for rapid and concomitant quantification of pro-inflammatory and pro-resolving polyunsaturated fatty acid metabolites.
- J. Chromatogr. B. *Analyt. Technol. Biomed. Life Sci.* 932, 123–133.
- Lee, A.Y. (2015). Recent progress in melasma pathogenesis. *Pigment Cell. Melanoma Res.* 28, 648–660.
- Lee, D.J., Park, K.C., Ortonne, J.P., and Kang, H.Y. (2012). Pendulous melanocytes: a characteristic feature of melasma and how it may occur. *Br. J. Dermatol.* 166, 684–686.
- Lo Cicero, A., Delevoye, C., Gilles-Marsens, F., Loew, D., Dingli, F., Guere, C., Andre, N., Vie, K., van Niel, G., and Raposo, G. (2015). Exosomes released by keratinocytes modulate melanocyte pigmentation. *Nat. Commun.* 6, 7506.
- Luo, C., Li, Y., Yang, L., Zheng, Y., Long, J., Jia, J., Xiao, S., and Liu, J. (2014a). Activation of Erk and p53 regulates copper oxide nanoparticle-induced cytotoxicity in keratinocytes and fibroblasts. *Int. J. Nanomedicine* 9, 4763–4772.
- Luo, N., Guan, Q., Zheng, L., Qu, X., Dai, H., and Cheng, Z. (2014b). Estrogen-mediated activation of fibroblasts and its effects on the fibroid cell proliferation. *Transl. Res.* 163, 232–241.
- Mahmoud, B.H., Ruvolo, E., Hexsel, C.L., Liu, Y., Owen, M.R., Kollias, N., Lim, H.W., and Hamzavi, I.H. (2010). Impact of long-wavelength UVA and visible light on melanocompetent skin. *J. Invest. Dermatol.* 130, 2092–2097.
- Makrantonaki, E., Adjaye, J., Herwig, R., Brink, T.C., Groth, D., Hultschig, C., Lehrach, H., and Zouboulis, C.C. (2006). Age-specific hormonal decline is accompanied by transcriptional changes in human sebocytes in vitro. *Aging Cell* 5, 331–344.
- Makrantonaki, E., Vogel, K., Fimmel, S., Oeff, M., Seltmann, H., and Zouboulis, C.C. (2008). Interplay of IGF-I and 17 $\beta$ -estradiol at age-specific levels in human sebocytes and fibroblasts in vitro. *Exp. Gerontol.* 43, 939–946.
- Makrantonaki, E., Ganceviciene, R., and Zouboulis, C. (2011). An update on the role of the sebaceous gland in the pathogenesis of acne. *Dermatoendocrinol* 3, 41–49.
- Mastrofrancesco, A., Ottaviani, M., Cardinali, G., Flori, E., Briganti, S., Ludovici, M., Zouboulis, C.C., Lora, V., Camera, E., and Picardo, M. (2017). Pharmacological PPARgamma modulation regulates sebogenesis and inflammation in SZ95 human sebocytes. *Biochem. Pharmacol.* 138, 96–106.
- McLeod, S.D., Ranson, M., and Mason, R.S. (1994). Effects of estrogens on human melanocytes in vitro. *J. Steroid Biochem. Mol. Biol.* 49, 9–14.
- Miot, L.D., Miot, H.A., Polettini, J., Silva, M.G., and Marques, M.E. (2010). Morphologic changes and the expression of alpha-melanocyte stimulating hormone and melanocortin-1 receptor in melasma

- lesions: a comparative study. *Am. J. Dermatopathol.* 32, 676–682.
- Muallem, M.M., and Rubeiz, N.G. (2006). Physiological and biological skin changes in pregnancy. *Clin. Dermatol.* 24, 80–83.
- Mukudai, S., Matsuda, K.I., Nishio, T., Sugiyama, Y., Bando, H., Hirota, R., Sakaguchi, H., Hisa, Y., and Kawata, M. (2015). Differential responses to steroid hormones in fibroblasts from the vocal fold, trachea, and esophagus. *Endocrinology* 156, 1000–1009.
- Murase, D., Hachiya, A., Amano, Y., Ohuchi, A., Kitahara, T., and Takema, Y. (2009). The essential role of p53 in hyperpigmentation of the skin via regulation of paracrine melanogenic cytokine receptor signaling. *J. Biol. Chem.* 284, 4343–4353.
- Muthusamy, V., and Piva, T.J. (2013). A comparative study of UV-induced cell signalling pathways in human keratinocyte-derived cell lines. *Arch. Dermatol. Res.* 305, 817–833.
- Nagy, I., Pivarcsi, A., Kis, K., Koreck, A., Bodai, L., McDowell, A., Seltmann, H., Patrick, S., Zouboulis, C.C., and Kemeny, L. (2006). Propionibacterium acnes and lipopolysaccharide induce the expression of antimicrobial peptides and proinflammatory cytokines/chemokines in human sebocytes. *Microbes Infect* 8, 2195–2205.
- Narzt, M.S., Pils, V., Kremslechner, C., Nagelreiter, I.M., Schosserer, M., Bessonova, E., Bayer, A., Reifschneider, R., Terlecki-Zaniewicz, L., Waidhofer-Sollner, P., et al. (2021). Epilipidomics of senescent dermal fibroblasts identify lysophosphatidylcholines as pleiotropic senescence-associated secretory phenotype (SASP) factors. *J. Invest. Dermatol.* 141, 993–1006.e15.
- Natale, C.A., Duperret, E.K., Zhang, J., Sadeghi, R., Dahal, A., O'Brien, K.T., Cookson, R., Winkler, J.D., and Ridky, T.W. (2016). Sex steroids regulate skin pigmentation through nonclassical membrane-bound receptors. *Elife* 5, e15104. <https://doi.org/10.7554/elife.15104>.
- Nikolakis, G., Seltmann, H., Hossini, A.M., Makrantonaki, E., Knolle, J., and Zouboulis, C.C. (2015). Ex vivo human skin and SZ95 sebocytes exhibit a homoeostatic interaction in a novel coculture contact model. *Exp. Dermatol.* 24, 497–502.
- Okazaki, M., Yoshimura, K., Uchida, G., and Harii, K. (2005). Correlation between age and the secretions of melanocyte-stimulating cytokines in cultured keratinocytes and fibroblasts. *Br. J. Dermatol.* 153 (Suppl 2), 23–29.
- Ortonne, J.P., Arellano, I., Berneburg, M., Cestari, T., Chan, H., Grimes, P., Hexsel, D., Im, S., Lim, J., Lui, H., et al. (2009). A global survey of the role of ultraviolet radiation and hormonal influences in the development of melasma. *J. Eur. Acad. Dermatol. Venereol.* 23, 1254–1262.
- Ottaviani, M., Flori, E., Mastrofrancesco, A., Briganti, S., Lora, V., Capitanio, B., Zouboulis, C.C., and Picardo, M. (2020). Sebocyte differentiation as a new target for acne therapy: an in vivo experience. *J. Eur. Acad. Dermatol. Venereol.* 34, 1803–1814.
- Passeron, T., Valencia, J.C., Bertolotto, C., Hoashi, T., Le Pape, E., Takahashi, K., Ballotti, R., and Hearing, V.J. (2007). SOX9 is a key player in ultraviolet B-induced melanocyte differentiation and pigmentation. *Proc. Natl. Acad. Sci. U S A.* 104, 13984–13989.
- Passeron, T., and Picardo, M. (2018). Melasma, a photoaging disorder. *Pigment Cell. Melanoma Res.* 31, 461–465.
- Picardo, M., Zompetta, C., De Luca, C., Cirone, M., Faggioni, A., Nazzaro-Porro, M., Passi, S., and Prota, G. (1991). Role of skin surface lipids in UV-induced epidermal cell changes. *Arch. Dermatol. Res.* 283, 191–197.
- Picardo, M., Ottaviani, M., Camera, E., and Mastrofrancesco, A. (2009). Sebaceous gland lipids. *Dermatoendocrinol* 1, 68–71.
- Picardo, M., Mastrofrancesco, A., and Biro, T. (2015). Sebaceous gland—a major player in skin homeostasis. *Exp. Dermatol.* 24, 485–486.
- Rabbani, P., Takeo, M., Chou, W., Myung, P., Bosenberg, M., Chin, L., Taketo, M.M., and Ito, M. (2011). Coordinated activation of Wnt in epithelial and melanocyte stem cells initiates pigmented hair regeneration. *Cell* 145, 941–955.
- Ranson, M., Posen, S., and Mason, R.S. (1988). Human melanocytes as a target tissue for hormones: in vitro studies with 1 alpha-25, dihydroxyvitamin D3, alpha-melanocyte stimulating hormone, and beta-estradiol. *J. Invest. Dermatol.* 91, 593–598.
- Regazzetti, C., De Donatis, G.M., Ghorbel, H.H., Cardot-Leccia, N., Ambrosetti, D., Bahadoran, P., Chignon-Sicard, B., Lacour, J.P., Ballotti, R., Mahns, A., and Passeron, T. (2015). Endothelial cells promote pigmentation through endothelin receptor B activation. *J. Invest. Dermatol.* 135, 3096–3104.
- Regazzetti, C., Sormani, L., Debayle, D., Bernerd, F., Tulic, M.K., De Donatis, G.M., Chignon-Sicard, B., Rocchi, S., and Passeron, T. (2018). Melanocytes sense blue light and regulate pigmentation through opsin-3. *J. Invest. Dermatol.* 138, 171–178.
- Rodriguez-Arambula, A., Torres-Alvarez, B., Cortes-Garcia, D., Fuentes-Ahumada, C., and Castanedo-Cazares, J.P. (2015). CD4, IL-17, and COX-2 are associated with subclinical inflammation in malar melasma. *Am. J. Dermatopathol.* 37, 761–766.
- Schalka, S. (2017). New data on hyperpigmentation disorders. *J. Eur. Acad. Dermatol. Venereol.* 31 (Suppl 5), 18–21.
- Schneider, M.R., and Paus, R. (2010). Sebocytes, multifaceted epithelial cells: lipid production and holocrine secretion. *Int. J. Biochem. Cell Biol.* 42, 181–185.
- Schneider, M.R., and Zouboulis, C.C. (2018). Primary sebocytes and sebaceous gland cell lines for studying sebaceous lipogenesis and sebaceous gland diseases. *Exp. Dermatol.* 27, 484–488.
- Sun, Q., Rabbani, P., Takeo, M., Lee, S.H., Lim, C.H., Noel, E.S., Taketo, M.M., Myung, P., Millar, S., and Ito, M. (2018). Dissecting Wnt signaling for melanocyte regulation during wound healing. *J. Invest. Dermatol.* 138, 1591–1600.
- Szollosi, A.G., Olah, A., Biro, T., and Toth, B.I. (2018). Recent advances in the endocrinology of the sebaceous gland. *Dermatoendocrinol* 9, e1361576.
- Tomita, Y., Maeda, K., and Tagami, H. (1992). Melanocyte-stimulating properties of arachidonic acid metabolites: possible role in postinflammatory pigmentation. *Pigment Cell Res* 5, 357–361.
- Torres-Alvarez, B., Mesa-Garza, I.G., Castanedo-Cazares, J.P., Fuentes-Ahumada, C., Oros-Ovalle, C., Navarrete-Solis, J., and Moncada, B. (2011). Histochemical and immunohistochemical study in melasma: evidence of damage in the basal membrane. *Am. J. Dermatopathol.* 33, 291–295.
- Toth, B.I., Olah, A., Szollosi, A.G., Czifra, G., and Biro, T. (2011). Sebocytes' makeup": novel mechanisms and concepts in the physiology of the human sebaceous glands. *Pflugers Arch.* 461, 593–606.
- Vachtenheim, J., and Borovansky, J. (2010). "Transcription physiology" of pigment formation in melanocytes: central role of MITF. *Exp. Dermatol.* 19, 617–627.
- Vibert, L., Aquino, G., Gehring, I., Subkankulova, T., Schilling, T.F., Rocco, A., and Kelsh, R.N. (2017). An ongoing role for Wnt signaling in differentiating melanocytes in vivo. *Pigment Cell. Melanoma Res.* 30, 219–232.
- Waldera Lupa, D.M., Kalfalah, F., Safferling, K., Boukamp, P., Poschmann, G., Volpi, E., Gotz-Rosch, C., Bernerd, F., Haag, L., Huebenthal, U., et al. (2015). Characterization of skin aging-associated secreted proteins (SAASP) produced by dermal fibroblasts isolated from intrinsically aged human skin. *J. Invest. Dermatol.* 135, 1954–1968.
- Wang, X., Liu, Y., Chen, H., Mei, L., He, C., Jiang, L., Niu, Z., Sun, J., Luo, H., Li, J., and Feng, Y. (2015). LEF-1 regulates tyrosinase gene transcription in vitro. *PLoS One* 10, e0143142.
- Wang, Y., Viennet, C., Robin, S., Berthon, J.Y., He, L., and Humbert, P. (2017). Precise role of dermal fibroblasts on melanocyte pigmentation. *J. Dermatol. Sci.* 88, 159–166.
- Yamaguchi, Y., Passeron, T., Watabe, H., Yasumoto, K., Rouzaud, F., Hoashi, T., and Hearing, V.J. (2007). The effects of dickkopf 1

on gene expression and Wnt signaling by melanocytes: mechanisms underlying its suppression of melanocyte function and proliferation. *J. Invest. Dermatol.* 127, 1217–1225.

Zouboulis, C.C., Seltmann, H., Neitzel, H., and Orfanos, C.E. (1999). Establishment and characterization of an immortalized human sebaceous gland cell line (SZ95). *J. Invest. Dermatol.* 113, 1011–1020.

Zouboulis, C.C., Picardo, M., Ju, Q., Kurokawa, I., Torocsik, D., Biro, T., and Schneider, M.R. (2016). Beyond acne: current aspects of sebaceous gland biology and function. *Rev. Endocr. Metab. Disord.* 17, 319–334.

## STAR★METHODS

### KEY RESOURCES TABLE

REAGENT or RESOURCE	SOURCE	IDENTIFIER
<b>Antibodies</b>		
Rabbit monoclonal anti-p21 Waf1/Cip1	Cell Signaling Technology	Cat# 2947; RRID: AB_823586
Rabbit monoclonal anti-phospho-p38 MAPK (Thr180/Tyr182)	Cell Signaling Technology	Cat#4511; RRID: AB_2139682
Polyclonal anti-rabbit IgG, HRP-linked secondary antibody	Cell Signaling Technology	Cat#7074; RRID: AB_2099233
Polyclonal anti-mouse IgG, HRP-linked secondary antibody	Cell Signaling Technology	Cat#7076; RRID: AB_330924
Mouse monoclonal anti-p53 (DO-7)	Agilent	Cat#M7001; RRID: AB_2206626
Mouse monoclonal anti-Tyrosinase (T311)	Santa Cruz Biotechnology	Cat#sc-20035; RRID: AB_628420
Rabbit polyclonal anti-GAPDH	Sigma-Aldrich	Cat#G9545; RRID: AB_796208
Mouse monoclonal anti-alphaSMA	Sigma-Aldrich	Cat#A5228; RRID: AB_262054
<b>Chemicals, peptides, and recombinant proteins</b>		
Quick Start™ Bradford 1x Dye Reagent	Bio-Rad Laboratories, Inc.	Cat#5000205
Prostaglandin D <sub>2</sub> (IUPAC Name: (Z)-7-[(1R,2R,5S)-5-hydroxy-2-[(E,3S)-3-hydroxyoct-1-enyl]-3-oxocyclopentyl]hept-5-enoic acid) (purity ≥ 98%)	Cayman Chemical	Cat#12010
Prostaglandin D <sub>2-d<sub>4</sub></sub> (IUPAC Name: (Z)-3,3,4,4-tetradeuterio-7-[(1R,2R,5S)-5-hydroxy-2-[(E,3S)-3-hydroxyoct-1-enyl]-3-oxocyclopentyl]hept-5-enoic acid) (purity ≥ 99%)	Cayman Chemical	Cat#312010
Prostaglandin E <sub>2</sub> (IUPAC Name: (Z)-7-[(1R,2R,3R)-3-hydroxy-2-[(E,3S)-3-hydroxyoct-1-enyl]-5-oxocyclopentyl]hept-5-enoic acid) (purity ≥ 98%)	Cayman Chemical	Cat#14010
Prostaglandin E <sub>2-d<sub>4</sub></sub> (IUPAC Name: (Z)-3,3,4,4-tetradeuterio-7-[(1R,2R,3R)-3-hydroxy-2-[(E,3S)-3-hydroxyoct-1-enyl]-5-oxocyclopentyl]hept-5-enoic acid) (purity ≥ 99%)	Cayman Chemical	Cat#314010
Prostaglandin F <sub>2<sub>x</sub></sub> (IUPAC Name: (Z)-7-[(1R,2R,3R,5S)-3,5-dihydroxy-2-[(E,3S)-3-hydroxyoct-1-enyl]cyclopentyl]hept-5-enoic acid) purity ≥ 98%	Cayman Chemical	Cat#16010
8-iso Prostaglandin F <sub>2<sub>x-d<sub>4</sub></sub></sub> (IUPAC Name: 9 $\alpha$ ,11 $\alpha$ ,15S-trihydroxy-(8 $\beta$ )-prosta-5Z,13E-dien-1-oic-3,3,4,4-d4 acid) (purity ≥ 99%)	Cayman Chemical	Cat#316350
Leukotriene B <sub>4</sub> (IUPAC Name: (5S,6Z,8E,10E,12R,14Z)-5,12-dihydroxyicos-6,8,10,14-tetraenoic acid) (purity ≥ 97%)	Cayman Chemical	Cat#20110
Leukotriene B <sub>4-d<sub>4</sub></sub> (IUPAC Name: (5S,6Z,8E,10E,12R,14Z)-6,7,14,15-tetradeuterio-5,12-dihydroxyicos-6,8,10,14-tetraenoic acid) (purity ≥ 99%)	Cayman Chemical	Cat#320110
Arachidonic acid (IUPAC Name: (5Z,8Z,11Z,14Z)-icos-5,8,11,14-tetraenoic acid) >95.0% (GC)	Sigma-Aldrich	Cat#10931
Formic acid for LC-MS LiChropur™, 97.5-98.5% (T)	Sigma-Aldrich	Cat#00940
Palmitic acid (IUPAC Name: hexadecanoic acid) (purity ≥ 97%)	Cambridge Isotope Laboratories Inc.	Cat#DLM-2895-0.1
Cyclic Pifithrin- $\alpha$ hydrobromide (IUPAC name: 2-(4-Methylphenyl)imidazo[2,1-b]-5,6,7,8-tetrahydrobenzothiazole hydrobromide)	Sigma-Aldrich	Cat#P4236
$\beta$ -Estradiol (IUPAC name: (17 $\beta$ )-estra-1,3,5(10)-triene-3,17-diol)	Sigma-Aldrich	Cat#E8875
<b>Critical commercial assays</b>		
Human IL-6 ELISA Kit	Diaclone SAS	Cat#950.030.192; 2 x 96 (pre-coated)
Human IL-8 ELISA Kit	Diaclone SAS	Cat#950.050.192; 2 x 96 (pre-coated)

(Continued on next page)

**Continued**

REAGENT or RESOURCE	SOURCE	IDENTIFIER
Human SCF ELISA Kit	Origene Technologies Inc.	Cat#EA102189
Human Endothelin ELISA Kit	Origene Technologies Inc.	Cat#EA100599
Human FGF1/FGF basic ELISA Kit	Origene Technologies Inc.	Cat#EA102179
Human AMSH(alpha-MSH) ELISA Kit	Wuhan Fine Biotech Co.	Cat#EH0792
Aurum™ Total RNA Mini kit	Bio-Rad Laboratories, Inc.	Cat#7326820
<b>Experimental Models: Cell Lines</b>		
Immortalized human SZ95 sebocytes	Zouboulis CC Laboratory	N/A
Primary cultures of dermal fibroblasts (NHFs)	This study	N/A
Primary cultures of melanocytes (NHMs)	This study	N/A
Primary cultures of keratinocytes (NHKs)	This study	N/A
ex vivo skin explants cultures	This Study	N/A
<b>Oligonucleotides</b>		
DKK1 forward GCCTCAGGATTGTGTTGTG	This study	N/A
DKK1 reverse TGTGAAGCCTAGAAGAATTACTG	This study	N/A
EDN1 forward GAAATCATTTGGTCAACACTC	This study	N/A
EDN1 reverse GGCATCTATTCACGGTCTCT	This study	N/A
b-FGF forward CTGGCTTCTAAATGTGTTACGGA	This study	N/A
b-FGF reverse GCCCAGGTCTGTTGGAT	This study	N/A
GAPDH forward TGCAACCACCAACTGCTTAGC	This study	N/A
GAPDH reverse GGCGTGGACTGTGGTCATGAG	This study	N/A
GDF15 forward CCCATGGTGCCTATTCAAAG	This study	N/A
GDF15 reverse GCTCATATGCAGTGGCAGTCTT	This study	N/A
IL-1 $\alpha$ forward CGCCAATGACTCAGAGGAAGA	This study	N/A
IL-1 $\alpha$ reverse AGGGCGTCATTCAAGATGAA	This study	N/A
IL-1 $\beta$ forward CTGAGCTGCCAGTGAAATG	This study	N/A
IL-1 $\beta$ reverse TTAGGGCCATCAGCTTCAAA	This study	N/A
IL-6 forward AGCCACTCACCTCTTCAGAACG	This study	N/A
IL-6 reverse GGTCAGGTTGTTCTGCCAG	This study	N/A
IL-8 forward CTTGGCAGCCTCCCTGATTC	This study	N/A
IL-8 reverse TTCTGTGTTGGCGCAGTGTG	This study	N/A
KGF forward CACCAGGCAGACAACAGACAT	This study	N/A
KGF reverse GTAAGTTCAGTTGCTGTGACGCT	This study	N/A
MITF forward ATGGACGACACCCTTCTC	This study	N/A
MITF reverse GGAGGATTGCTAACAAAGTG	This study	N/A
MMP1 forward CTGGCCACAACTGCCAAATG	This study	N/A
MMP1 reverse CTGCCCCCTGAACAGCCCAGTACTTA	This study	N/A
NRG1 forward AGCCTCACTGAAGGAGCAT	This study	N/A
NRG1 reverse ACTCCCCCTCCATTCACACAG	This study	N/A
POMC forward CTCCCGAGACAGAGCCTCA	This study	N/A
POMC reverse ACTTCCATGGAGGCCTGAAG	This study	N/A
SCF forward AAGAGGATAATGAGATAAGTATGTTGC	This study	N/A
SCF reverse TTACCAGCCAATGTACGAAAGT	This study	N/A
$\alpha$ -SMA forward GCAGCCCCAGCCAAGCACTGT	This study	N/A
$\alpha$ -SMA reverse TGGGAGCATCGTCCCCAGCA	This study	N/A
SOX9 forward CACGCTGACCACGCTGAG	This study	N/A

(Continued on next page)

**Continued**

REAGENT or RESOURCE	SOURCE	IDENTIFIER
SOX9 reverse TGCTGCTGCTCGCTGTAG	This study	N/A
TYR forward AGCATCCTTCTTCCTCCCTG	This study	N/A
TYR reverse GCTGAAATTGGCAGTTCTATCC	This study	N/A
VEGF forward GTTGACCTCCTCCATCC	This study	N/A
VEGF reverse TTCTCTGCCTCCACAATG	This study	N/A
WIF1 forward TACGAAGCCAGCCTCATAC	This study	N/A
WIF1 reverse TGTCGGAGTTCACCAGATG	This study	N/A
WNT 5A forward AGCACGACGAAGCAACCTG	This study	N/A
WNT 5A reverse GCCCTCTCCACAAAGTGAACAG	This study	N/A
<b>Software and algorithms</b>		
CFX Manager™ Software	Bio-Rad Laboratories, Inc.	NA
NineAlliance Software	Uvitec	NA
<b>Other</b>		
Sebomed Basal Medium	Merck	Cat#F8205
Dulbecco's Modified Eagle's Medium High Glucose	EuroClone	Cat#ECB7501L
Fetal Bovine Serum Characterized (FBS)	HyClone	Cat#SH30071.03
Cascade Biologics™ Medium 254	Thermo Fisher Scientific	Cat#M-254-500

## RESOURCE AVAILABILITY

### Lead contact

Further information and requests for resources and reagents should be directed to and will be fulfilled by the corresponding authors, Mauro Picardo ([mauro.picardo@ifo.gov.it](mailto:mauro.picardo@ifo.gov.it)) and Enrica Flori ([enrica.flori@ifo.gov.it](mailto:enrica.flori@ifo.gov.it)).

### Materials availability

All materials are available from the corresponding authors upon reasonable request.

### Data and code availability

Data reported in this paper will be shared by the lead contact upon request. This paper does not report original code. Any additional information required to reanalyze the data reported in this paper is available from the lead contact upon request.

## EXPERIMENTAL MODEL AND SUBJECT DETAILS

### Cells

Immortalized human SZ95 sebocytes ([Zouboulis et al., 1999](#)), showing morphologic, phenotypic and functional characteristics of normal human sebocytes, were cultured in Sebomed® basal medium, supplemented with 10% FBS, L-glutamine (2mM), penicillin/streptomycin (100 µg/ml), recombinant human epidermal growth factor (5 ng/ml) and CaCl<sub>2</sub> (1 mM) in a humidified atmosphere containing 5% CO<sub>2</sub> at 37°C. Cell line were routinely tested for Mycoplasma detection. For SZ95-SF sebocytes were maintained without FBS. Primary cultures of dermal fibroblasts (NHF) and melanocytes (NHMs) were isolated from neonatal foreskins (at least n=5 donors) after mechanical dissection of skin biopsies. In brief, NHFs were maintained in DMEM supplemented with 10% FBS, penicillin/streptomycin (100 µg/ml) and used between passage 2 and 10. NHMs were grown in M254 medium with Human Melanocyte Growth Supplements and penicillin/streptomycin (100 µg/ml) and used between passage 2 and 10 ([Flori et al., 2011; Briganti et al., 2014](#)).

### Human subjects

Healthy skin was obtained from perilesional areas of disposable donors after dermatological interventions. 10 female patients with facial melasma (42±8 years old) were enrolled from the San Gallicano

Dermatological Ambulatory for sebum collection. Sebum samples were collected using Sebutapes<sup>TM</sup> (Cu-derm, Dallas, TX, USA) ([Camera et al., 2016](#)). Skin was cleaned gently with 70% ethanol and tapes were applied and hold for 30 min. Sebutapes<sup>TM</sup> were stored at -80 °C until processing.

Participants gave written informed consent. The Institutional Research Ethics Committee (IFO) approval was obtained to collect samples of human material for research. The study adhered to the Declaration of Helsinki principle guidelines.

## METHODS DETAILS

### UVA irradiation treatment of SZ95 sebocytes and NHFs

SZ95 were irradiated with increasing doses of UVA (2 J/cm<sup>2</sup>, 5 J/cm<sup>2</sup> and 8 J/cm<sup>2</sup>), according to the scheme in [Figure 1A](#). NHFs were incubated in medium without phenol-red and irradiated with UVA at the dose of 5 J/cm<sup>2</sup>, according to the scheme in [Figure 5A](#). Control cells were treated identically but without UVA exposure. The Bio-Sun irradiation apparatus (Vilbert Lourmat, Marne-la Vallée, France) was employed. The UVA lamps in the illuminator emit ultraviolet rays between 355 nm and 375 nm, with peak luminosity at 365 nm. UVA was supplied by a closely spaced array of four UVA lamps which delivered uniform irradiation at the distance of 10 cm. Based on a programmable microprocessor, the Bio-Sun system constantly monitors the UV light emission. The irradiation stops automatically when the energy received matches the programmed energy (range of measure: 0 to 9,999 J/cm<sup>2</sup>). S in the text indicates SZ95 exposed to a single UVA treatment, whereas R stands for SZ95 exposed to repetitive UVA.

### Cell treatments

Cell treatments are indicated in [Tables 1, 2, and 3](#).

### Morphologic analysis by inverted phase contrast microscope

Living cell cultures were observed daily and images were captured by an inverted phase microscope (Axiovert 40C, Zeiss, Oberkochen, Germany) equipped with a digital camera.

### RNA extraction and quantitative real-time PCR

Total RNA was isolated using the Aurum<sup>TM</sup> Total RNA Mini kit (Bio-Rad Laboratories Srl, Milan, Italy). Total RNA samples were stored at -80°C until use. Following DNase I treatment, cDNA was synthesized using a mix of oligo-dT and random primers and RevertAid<sup>TM</sup> First Strand cDNA synthesis kit (Thermo Fisher Scientific, Monza (MB) Italy) according to the manufacturer's instructions. Quantitative real time RT-PCR was performed in a total volume of 10 µl with SYBR Green PCR Master Mix (Bio-Rad Laboratories Srl) and 200 nM concentration of each primer. Reactions were carried out in triplicates using a CFX96 Real Time System (Bio-Rad Laboratories Srl). Melt curve analysis was performed to confirm the specificity of the amplified products. Expression of mRNA (relative) was normalized to the expression of GAPDH mRNA by the change in the Δ cycle threshold (ΔC<sub>t</sub>) method and calculated based on 2<sup>-ΔC<sub>t</sub></sup>.

### Protein determination by sandwich enzyme-linked immunosorbent assay (ELISA)

α-MSH, SCF, b-FGF, EDN1, IL-6 and IL-8 protein level was determined using commercially available ELISA kit, according to the manufacturer's instructions. The measurement was performed in duplicate for each sample. The absorbance at 450 nm was recorded using a DTX880 Multimode Detector spectrophotometer (Beckman Coulter, Milan, Italy). For *in vitro* experiments, culture supernatants were collected and centrifuged for removal of cell detritus. Aliquots were stored at -80°C until use. The results were normalized for the number of cells contained in each sample. As regard sebum samples, protein extracts were used for the analysis. The results were normalized for the squalene content of each sample. Squalene is specific of sebum secretion, therefore squalene amount can be considered representative of sebum content ([Picardo et al., 2009](#)).

### Assessment of pro-inflammatory lipid mediators' cellular concentrations

Prostaglandins (PGD2, PGE2, PGF2α), LTB4, and AA release in cell media were measured by HPLC\MS\MS. Sebocytes supernatants (1ml) were added with 10 µL of IS solution (PGD2-d4 PGE2-d4, LTB4-d4, and d17PA 1 µM), 100 µL of 0.2% FA, and 3 ml of ethyl acetate. Samples were vortexed and centrifuged at 20,000 g for 20 min at 4 °C. The extraction procedure was repeated twice and the clear supernatants were collected and evaporated under N2. After evaporation, the samples were dissolved with 30 µL of

MeOH containing BHT (1 mM) and stored at  $-80^{\circ}\text{C}$  before LC–MS/MS analysis. Chromatographic separation was carried out using the Agilent Technologies 1200 HPLC Liquid Chromatography System (Palo alto, CA, USA) with a C18 column (Symmetry, 3.5  $\mu\text{m}$ , 100 mm  $\times$  2.1 mm, Waters) (Furugen et al., 2015; Le Faouder et al., 2013). Briefly, the mobile phase flow rate was 0.2 mL/min. Mobile phase A consisted of acetonitrile–water–formic acid (20:80:0.1, v/v/v), and mobile phase B consisted of acetonitrile–formic acid (100:0.1, v/v). Mobile phase B was increased from 0 to 100% in a linear gradient over 6 min and maintained at 100% until 10 min. Mobile phase B was then decreased to 0% from 10 to 11 min and maintained at 0% until 22 min. The column temperature was maintained at  $40^{\circ}\text{C}$ . The injection volume was 10  $\mu\text{L}$ . The overall run time was 25 min. Negative ion electrospray tandem mass spectrometry was carried out with an Agilent Technologies triple quadrupole 6400 mass spectrometer at unit resolution with multiple reaction monitoring (MRM) performed by monitoring the following transitions: PGD2 351  $\rightarrow$  233; PGD2-d4 (IS for PGD2) 355  $\rightarrow$  233; PGE2 351  $\rightarrow$  315; PGE2-d4 (IS for PGE2) 355  $\rightarrow$  319; PGF $2\alpha$  353  $\rightarrow$  193; PGF $2\alpha$ -d4 (IS for PGF $2\alpha$ ) 357  $\rightarrow$  197; LTB4 335  $\rightarrow$  195; LTB4-d4 (IS for LTB4) 339  $\rightarrow$  197; AA 303  $\rightarrow$  303; d17-palmitic acid (IS for AA 272  $\rightarrow$  272). For each compound to be quantified, an internal standard was selected and a linear curve was generated where the ratio of analyte standard peak area to internal standard peak area was plotted versus the amount of analyte standard. The results are calculated as nM/ $10^6$  cells and then reported as % variation vs control values.

### Western blot analysis

Cells were lysed in denaturing conditions supplemented with a protease inhibitor cocktail (Roche, Mannheim, Germany), then sonicated. Total cell lysates were clarified by centrifugation at 12,000 rpm for 10 minutes at  $4^{\circ}\text{C}$  and then stored at  $-80^{\circ}\text{C}$  until analysis. Following spectrophotometric protein measurement, equal amounts of protein were resolved on acrylamide SDS-PAGE, transferred onto nitrocellulose membrane (Amersham Biosciences, Milan, Italy). Protein transfer efficiency was checked with Ponceau S staining (Sigma-Aldrich). Membranes were first washed with PBS and then blocked with 5% fat-free dry milk in PBS with 0.05% Tween-20 for 1 h at room temperature and then treated overnight at  $4^{\circ}\text{C}$  with anti-p53 (1:1000), anti-p21 (1:1000), anti-phospho-p38 (1:1000), anti-Tyrosinase (1:1000), and anti- $\alpha$ -SMA (1:1000). A secondary anti-mouse IgG HRP-conjugated antibody (1:3000) and anti-rabbit IgG HRP-conjugated antibody (1:8000) were used. Antibody complexes were visualized using ECL (Santa Cruz). A subsequent hybridization with anti-GAPDH (1:5000) was used as a loading control. Protein levels were quantified by measuring the optical densities of specific bands using UVI-TEC Imaging System (Cambridge, UK). Control value was taken as one fold in each case.

### Tyrosinase assay

Tyrosinase activity was estimated by measuring the rate of L-DOPA (3,4-dihydroxyphenylalanine) oxidation (Flori et al., 2011). Cells were treated according to the experimental design. The cells were solubilized with 1% Triton X100 and lysates were clarified by centrifugation at 10000 g for 10 min. After protein quantification by Bradford reagent (Sigma-Aldrich) and adjustment of protein concentration with lysis buffer, 80  $\mu\text{l}$  aliquots of each lysate (each containing the same amount of protein) were placed in the wells of a 96-well plate, with 20  $\mu\text{l}$  of 5 mM L-DOPA. Absorbance was measured spectrophotometrically at 475 nm following a 20-min incubation period at  $37^{\circ}\text{C}$ , using a DTX880 Multimode Detector spectrophotometer (Beckman Coulter). Measurement was repeated five times.

### Melanin content determination

For intracellular melanin content determination, cell pellets were dissolved in 1 M NaOH and incubated at  $60^{\circ}\text{C}$  for 1 h. Total melanin in the cell suspension was determined with a  $\mu$ QUANT spectrophotometer (BIO-TEK Instruments Inc., Winooski, VT, USA) by reading the absorbance at 405 nm. Melanin content was calculated by interpolating the results with a standard curve, generated by the absorbance of known concentrations of synthetic melanin. The results were normalized by protein levels in each sample.

### Lipid depletion

For the lipid depletion, the collected SZ95 medium was treated with Cleanascite™ (Biotech Support Group, North Brunswick, NJ), a commercially available lipid removal and clarification reagent. This reagent is a saline suspension of a solid-phase non-ionic adsorbent (pH 8.0) that selectively removes lipids from biological samples. Immediately prior to use, the Cleanascite reagent was completely resuspended by gentle shaking. Cleanascite was added to the collected SZ95 medium in a ratio 1:4 and mixed for 10 min at

room temperature by gentle shaking. Following centrifugation (16000g) for 1 min at 4 °C, the supernatant was carefully decanted into a clean collection vial and used for experiments.

### Skin explants and co-culture experiments

Healthy skin was obtained from perilesional areas of disposable donors after dermatological interventions. After subcutaneous fat excision skin samples were cut with a punch of 4 mm diameter, and cultured, with the dermis downside, on transwell permeable supports (6.5 mm diameter, 0.4 µm pore size) into standard well plates at the air-liquid interface. Skin explants were cultured for 4 days in conditioned medium of SZ95 sebocytes sham-irradiated or repeatedly irradiated (UVA 5J/cm<sup>2</sup>) and collected 48h after the last irradiation. For co-culture experiments, skin explants were placed on petri dishes seeded with SZ95 sebocytes irradiated with UVA (5J/cm<sup>2</sup>) for four times and maintained in culture until 48h after the last irradiation (see schemes in Figures 7A and 7B).

### Immunohistochemical analysis

At the end of the treatments skin explants were fixed in formalin and embedded in paraffin. Paraffin sections were routinely stained with hematoxylin and eosin (H&E) for histomorphological analysis and treated for immunostaining. Melanin content was detected by Fontana-Masson staining. SCF expression was evaluated using a polyclonal antibody (sc-9132, Santa Cruz Biotechnology Inc) and visualized with immunoperoxidase technique. Staining signals were analyzed by recording images using a CCD camera (Zeiss, Oberkochen, Germany).

### Protein and squalene extraction from sebutape

Proteins extraction was performed by scraping one tape in 150 µl of a buffer containing Tris HCl pH=6.8; SDS 10%; protease inhibitor. The extract was centrifuged (10 min, 10.000 g) and supernatant aliquots were frozen at -80°C until analysis. Squalene was extracted from the Sebutapes™ as previously described (Ottaviani et al., 2020). Briefly, ethanol (Merck, Darmstadt, Germany) containing 0.025% of butylhydroxytoluene (BHT; Sigma-Aldrich, Milan, Italy) to prevent oxidation was used for the extraction. Deuterated squalene (d6-SQ) was added as internal standard. Lipid extract was further cleaned-up by liquid-liquid extraction with ethyl acetate. The dried extract was then dissolved in acetone/methanol/isopropanol (40/40/20 v/v) mixture and stored at -80°C until analysis.

### Squalene GC-MS analysis

Squalene (SQ) content in sebum samples was determined by gas chromatography-mass spectrometry (Mastrofrancesco et al., 2017). The chromatographic separation was performed on a HP-5MS (Agilent Technologies, Santa Clara, CA, USA) capillary column (30m x 0,25 µm x 0,25 µm), using helium as the carrier gas. An oven temperature gradient from 80 °C to 280 °C at 6 °C/min and then to 310°C at 4°C/min was used. The injector and the GC-MS transfer lines were kept at 260°C and 230°C, respectively. Samples were acquired in single ion monitoring (SIM) coupled to scan mode utilizing electron impact (EI) mass spectrometry. The identity of the detected SQ was verified by the comparison with authentic standard and the match with library spectral data. Calibration curve, built against the deuterated IS d6-SQ, was used for the quantitative analysis (selected ions: SQ m/z 69.1; d6-SQ m/z 75.1).

## QUANTIFICATION AND STATISTICAL ANALYSIS

Data were represented as mean ± SD of three independent using at least three different donors for primary cells. Statistical significance was assessed using paired Student's t-test. The minimal level of significance was  $p \leq 0,05$ .